

# Exact and efficient solutions of the LMC Multitask Gaussian Process model

Olivier Truffinet<sup>1 2</sup>   Karim Ammar<sup>1</sup>   Jean-Philippe Argaud<sup>3</sup>   Bertrand Bouriquet<sup>4</sup>

October 19, 2023

<sup>1</sup>CEA/DES/ISAS/DM2S/SERMA/LPEC, Paris-Saclay University

<sup>2</sup>Corresponding author, [olivier.truffinet@gmail.com](mailto:olivier.truffinet@gmail.com)

<sup>3</sup>EDF R&D

<sup>4</sup>EDF



### Abstract

The Linear Model of Co-regionalization (LMC) is a very general model of multitask gaussian process for regression or classification. While its expressivity and conceptual simplicity are appealing, naive implementations have cubic complexity in the number of datapoints and number of tasks, making approximations mandatory for most applications. However, recent work has shown that under some conditions the latent processes of the model can be decoupled, leading to a complexity that is only linear in the number of said processes. We here extend these results, showing from the most general assumptions that the only condition necessary to an efficient exact computation of the LMC is a mild hypothesis on the noise model. We introduce a full parametrization of the resulting *projected LMC* model, and an expression of the marginal likelihood enabling efficient optimization. We perform a parametric study on synthetic data to show the excellent performance of our approach, compared to an unrestricted exact LMC and approximations of the latter. Overall, the projected LMC appears as a credible and simpler alternative to state-of-the art models, which greatly facilitates some computations such as leave-one-out cross-validation and fantasization.



# 1 Introduction

Multi-Outputs Gaussian Processes (MOGP) are a popular tool for the learning – both supervised and unsupervised – of linearly correlated quantities. They find use in many fields : earth and climate sciences, robotics, surrogate modeling... Some very recent successful applications include modeling of electrical motors (Wen, 2021, [25]), indoor localization (Tang, 2022, [23]), solar power prediction (Dahl, 2019, [7]), and inverse problem resolution for a centrifugal pump blade (Zhang, 2020, [26]). They even provide full paradigms for tasks such as uncertainty quantification (Bilionis, 2013, [2]) and Bayesian optimization (Maddox, 2021, [17]). As described in a survey of MOGPs from 2018 by Liu (2018, [15]), the vast majority of models operating in the most straightforward setup – supervised learning of several tasks, all akin to each other and treated in the same fashion – fall into two main categories: this of *convolutional GPs* and this of *linearly correlated GPs*. The latter can essentially be grouped under the term “*Linear model of co-regionalization*” (LMC).

The LMC stems from a very natural idea, this of modelizing all observed outputs as linear combinations of common unobserved and independant gaussian processes. From an equivalent perspective, the outputs can also be viewed as a vector-valued function, which follows a multidimensional gaussian process with vectorial mean function and matricial kernel function (Alvarez, 2012, [1]); then the equations of single-output GPs apply to this model, modulo a flattening of some matricial quantities, and posteriors and likelihood can be computed exactly. However, **this procedure scales as  $\mathcal{O}((np)^3)$**  both for training and inference, making it intractable in most cases. Several methods have therefore been developed to circumvent this limitation, which rely on two complementary approaches: either **restricting the model to some particular case that is more amenable to computation**, reducing its expressivity, or **approximating some of its parts**, thus degrading its accuracy. The first category includes the *intrinsic coregionalization model* (ICM), sometimes referred to as Multi-Task Gaussian Process (Bonilla, 2007, [4]), where all latent processes are restricted to have the same kernel, and both the Orthogonal Instantaneous Linear Mixing Model (OILMM, Bruinsma, 2020, [6]) and the Generalized Probabilistic Principal Component Analysis (GPPCA, Gu, 2021, [9]), in which the mixing matrix encoding correlations between outputs is constrained to be orthogonal. Models of the second category often resort to *variational approaches* (Bonilla, 2019, [5]), which introduce an approximate form for the posterior of latent processes and optimize a lower bound of the marginal log-likelihood instead of this quantity itself; they include in particular the pioneer Semiparametric Latent Factor Model (Cowell, 2005, [24]) and the Collaborative multi-output Gaussian Process (Nguyen, 2014, [18]). We emphasize that all of the cited methods are *subcases or approximations* of the LMC, not distinct models that would extend its generality.

The present work generalizes two recent publications introducing respectively the OILMM and the GPPCA (see above paragraph). As their authors point it out, these models are subcases of the LMC where assumptions are made on the noise model, and more importantly on the mixing matrix, which is constrained to have orthogonal or orthonormal columns. However, it happens that **this assumption of orthogonality is unnecessary**: exact and convenient computation of the model can be carried without it, at the expense of a slightly more complex treatment of the noise. This is the main finding motivating the present article.

The main contributions of this paper are as follows:

- We write general expressions for posteriors of the LMC variables at the level of latent processes, and show how they can be efficiently computed if a specific condition on the noise model is enforced;
- We find a general form for noise matrices enforcing this condition, compute and optimize the marginal log-likelihood of the model given this parametrization;
- We demonstrate the validity of our approach by comparing the resulting projected LMC to its exact counterpart and to concurrent approximations; in particular, we undertake a parametric study on synthetic data to assess the effects of the noise hypothesis in various setups.

## 2 Background and notations

A generic LMC model is specified by  $\mathbf{y} = \mathbf{H}\mathbf{u} + \boldsymbol{\epsilon}$ , with  $\mathbf{H}$  a  $p \times q$  mixing matrix without any specific property,  $\mathbf{u} = (u_1, \dots, u_q)^T \in \mathbb{R}^q$  such that  $u_i \sim \mathcal{GP}(0, k_i)$  and priors of the  $u_i$ 's are mutually independant, and  $\boldsymbol{\epsilon} \sim \mathcal{N}(0, \boldsymbol{\Sigma})$ , with  $\boldsymbol{\Sigma} \in \mathbb{R}^{p \times p}$  the inter-task noise matrix which is symmetric but not necessarily diagonal. We also note  $\mathbf{X} = (X_{ij})_{1 \leq i \leq d}^{1 \leq j \leq n}$  the matrix of  $d$ -dimensional input points,  $\mathbf{Y} = (Y_{ij})_{1 \leq i \leq p}^{1 \leq j \leq n}$  this of the  $p$  data outputs,  $\mathbf{U} = (U_{ij})_{1 \leq i \leq q}^{1 \leq j \leq n}$  the values of the  $q$  latent processes at observation points,  $\text{vec}(\mathbf{M})$  the vectorization of the matrix  $\mathbf{M}$  (i.e its column-wise unfolding),  $\mathbf{M}_{\mathbf{v}} = \text{vec}(\mathbf{M}^T)$ ,  $\mathbf{x}_*$  a test point for prediction,  $\hat{\Phi}$  the probabilistic estimator of random variable  $\Phi$ ,  $\mathbf{k}_{i*} = (k_i(\mathbf{x}_*, \mathbf{x}_j))_{1 \leq j \leq n}$  and  $k_{i**} = k_i(\mathbf{x}_*, \mathbf{x}_*)$  the train/test covariance vector



and test-test variance for kernel  $i$ ,  $\text{Diag}(\mathbf{K}_i)$  the block-diagonal matrix where the  $i$ -th block is the kernel matrix  $\mathbf{K}_i$  (the subscript indicating iteration on  $i$  is omitted), and  $\otimes$  the Kronecker product. For simplicity, we restrict ourselves to the case of zero-mean GPs: the case of a general sum-of-regressors mean function, significantly more convoluted and useful only in peculiar setups, will be the matter of future work.

The naive exact implementation of the LMC is then written (Alvarez, 2012, [1]):

$$p(\mathbf{y}_*|\mathbf{Y}) = \mathcal{N}(\mathbf{k}_*^T \mathcal{K}^{-1} \mathbf{Y}_v, \mathbf{k}_{**} - \mathbf{k}_*^T \mathcal{K}^{-1} \mathbf{k}_*) \quad (1)$$

$$-2 \log p(\mathbf{Y}) = \mathbf{Y}_v^T \mathcal{K}^{-1} \mathbf{Y}_v + \log |\mathcal{K}| + \frac{np}{2} \log \pi \quad (2)$$

for respectively predictions at a new point  $\mathbf{y}_*$  and the marginal log-likelihood, with  $\mathcal{K} = (\mathbf{H} \otimes \mathbf{I}_n) \text{Diag}(\mathbf{K}_i) (\mathbf{H}^T \otimes \mathbf{I}_n) + \Sigma \otimes \mathbf{I}_n$  the noise-added cross-tasks covariance matrix. This is formally equivalent to the computation of a single-output GP, but with the burden of handling an  $(np \times np)$  matrix in all operations.

### 3 Latent-revealing expressions of LMC estimators

We now present new exact expressions for the LMC, which highlight its low-rank structure.

#### 3.1 Posteriors

**Proposition 1.** *The posterior  $p(\mathbf{U}_v|\mathbf{Y})$  of the latent processes  $\mathbf{U}$  at the training points is gaussian with mean and variance:*

$$\mathbb{E}(\mathbf{U}_v|\mathbf{Y}) = [\text{Diag}(\mathbf{K}_i^{-1}) + \mathbf{H}^T \Sigma^{-1} \mathbf{H} \otimes \mathbf{I}_n]^{-1} \cdot \text{vec}(\mathbf{Y}^T \Sigma^{-1} \mathbf{H}) \quad (3)$$

$$\mathbb{V}(\mathbf{U}_v|\mathbf{Y}) = (\text{Diag}(\mathbf{K}_i^{-1}) + \mathbf{H}^T \Sigma^{-1} \mathbf{H} \otimes \mathbf{I}_n)^{-1} \quad (4)$$

**Remark 1.** *It can be noted that 3 is only a blockwise version of the result (2.116) of Bishop’s textbook (2006, [3]) for the conditional law of a linear combination of joint gaussian variables, applied here with  $\mathbf{x} = \mathbf{U}_v$ ,  $\mathbf{A} = \mathbf{H}$ ,  $\mathbf{L} = \Sigma^{-1}$ ,  $\mathbf{\Lambda} = \text{Diag}(\mathbf{K}_i^{-1})$  and  $\boldsymbol{\mu} = \mathbf{0}$ ,  $\mathbf{b} = \mathbf{0}$ . The only difference is that the vectors  $\mathbf{x}$  and  $\mathbf{y}$  in the above manual contain one value per “task”, whereas our vectors  $\mathbf{U}_v$  and  $\mathbf{Y}_v$  contain gaussian subvectors of size  $n$ .*

Let  $\hat{\mathbf{y}}_*$  be our estimator for  $\mathbf{Y}$  at test point  $\mathbf{x}_*$  and  $\hat{\mathbf{u}}_*$  this for  $\mathbf{U}$ .  $\mathbf{H}$  being considered deterministic, we have  $p(\hat{\mathbf{y}}_*|\mathbf{Y}) = p(\mathbf{H}\hat{\mathbf{u}}_*|\mathbf{Y}) = \mathcal{N}(\mathbf{H}\mathbb{E}(\hat{\mathbf{u}}_*|\mathbf{Y}), \mathbf{H}\mathbb{V}(\hat{\mathbf{u}}_*|\mathbf{Y})\mathbf{H}^T)$ . Therefore, the only quantity still required for prediction is  $p(\hat{\mathbf{u}}_*|\mathbf{Y})$ . This is done in the following proposition:

**Proposition 2.**  *$p(\hat{\mathbf{u}}_*|\mathbf{Y})$  is gaussian with respective mean and variance:*

$$\mathbb{E}(\hat{\mathbf{u}}_*|\mathbf{Y}) = \mathfrak{K} [\mathbb{K} + (\mathbf{H}^T \Sigma^{-1} \mathbf{H})^{-1} \otimes \mathbf{I}_n]^{-1} \cdot \text{vec}(\mathbf{Y}^T \Sigma^{-1} \mathbf{H} (\mathbf{H}^T \Sigma^{-1} \mathbf{H})^{-1}) \quad (5)$$

$$\mathbb{V}(\hat{\mathbf{u}}_*|\mathbf{Y}) = \mathbf{k}_d - \mathfrak{K} [\mathbb{K} + (\mathbf{H}^T \Sigma^{-1} \mathbf{H})^{-1} \otimes \mathbf{I}_n]^{-1} \mathfrak{K} \quad (6)$$

with further notations  $\mathbb{K} = \text{Diag}(\mathbf{K}_i)$ ,  $\mathfrak{K} = \text{Diag}(\mathbf{k}_{i*})$  and  $\mathbf{k}_d = \text{Diag}(k_{i**})$  for compacity.

These expressions are very close to a block-diagonal version of a single-output GP. Two quantities stand out from them: a term  $(\mathbf{H}^T \Sigma^{-1} \mathbf{H})^{-1}$  which seems to play the role of a noise for the latent processes, and a matrix  $(\mathbf{H}^T \Sigma^{-1} \mathbf{H})^{-1} \mathbf{H}^T \Sigma^{-1} \mathbf{Y}$  which appears to act as a  $q$ -dimensional summary of the data. We therefore set the following notations:

**Definition 1.** *We note  $\Sigma_P = (\mathbf{H}^T \Sigma^{-1} \mathbf{H})^{-1}$  and  $\mathbf{T} = (\mathbf{H}^T \Sigma^{-1} \mathbf{H})^{-1} \mathbf{H}^T \Sigma^{-1} = \Sigma_P \mathbf{H}^T \Sigma^{-1}$ .*

#### 3.2 Likelihood

In the same vein as the above expressions, the following formula from Bruinsma expresses the likelihood at the level of the latent processes rather than the observable tasks. Remarkably,  $\Sigma_P$  and  $\mathbf{T}\mathbf{Y}$  also play a major role here.

**Proposition 3.** *The likelihood of the data can be decomposed as the likelihood of the projected data multiplied by a corrective term accounting for projection loss, independent of the latent processes:*

$$p(\mathbf{Y}) = \prod_{j=1}^n \frac{\mathcal{N}(\mathbf{Y}_j|\mathbf{0}, \Sigma)}{\mathcal{N}(\mathbf{T}\mathbf{Y}_j|\mathbf{0}, \Sigma_P)} \times \int p(\mathbf{U}) \prod_{j=1}^n \mathcal{N}(\mathbf{T}\mathbf{Y}_j|\mathbf{U}_j, \Sigma_P) d\mathbf{U} \quad (7)$$

(where  $\mathbf{Y}_j$ ,  $\mathbf{U}_j$  denote the columns of  $\mathbf{Y}$  and  $\mathbf{U}$  respectively).

The derivation of (7), taken from the OILMM paper, is quite clever and requires preable investigation of  $\Sigma_P$  and  $\mathbf{T}\mathbf{Y}$ . However, a similar expression<sup>1</sup> can be derived from elementary considerations and is displayed in Annex B.

<sup>1</sup>But slightly less convenient as it doesn’t boil down to MLLs of single-output GPs.



### 3.3 Decoupled expressions

We have derived so far exact expressions for all quantities of the model; but these expressions are not necessarily cheaper to compute than their "naive" counterpart (1). Looking at  $\mathbb{E}(\hat{\mathbf{u}}_*|\mathbf{Y})$  and  $\mathbb{V}(\hat{\mathbf{u}}_*|\mathbf{Y})$ , it appears that they consist in products of block-diagonal matrices and a single large  $nq \times nq$  matrix,  $\mathcal{K}^{-1} = [\text{Diag}(\mathbf{K}_i) + \Sigma_{\mathbf{P}} \otimes \mathbf{I}_n]^{-1}$ . By resorting to the "trick"  $p(\hat{\mathbf{y}}_*|\mathbf{Y}) = \mathcal{N}(\mathbf{H}\mathbb{E}(\hat{\mathbf{u}}_*|\mathbf{Y}), \mathbf{H}\mathbb{V}(\hat{\mathbf{u}}_*|\mathbf{Y})\mathbf{H}^T)$ , we have reduced complexity from  $O(n^3p^3)$  to  $O(n^3q^3)$ , but there is a much more crucial observation: **a necessary and sufficient condition for  $\mathcal{K}$  to be block-diagonal is that  $\Sigma_{\mathbf{P}}$  be diagonal**. We frame this condition as of now given its importance in the rest of the article:

**Definition 2.** We say that  $\Sigma$  is a diagonally projectable noise for  $\mathbf{H}$ , abbreviated as DPN, if  $\mathbf{H}^T\Sigma^{-1}\mathbf{H}$  is diagonal.

It follows immediately that if the DPN condition is verified, the estimators of prop. 2 decouple: we can express the component  $p(\hat{u}_{i*}|\mathbf{Y})$  in function of only  $k_i$  and a specific projection of  $\mathbf{Y}$  of size  $n \times q$ . The computational cost then falls to  $O(n^3q)$  – also minding that the cubic complexity in  $n$  can be reduced by resorting to any approximation method for single-output GPs, such as inducing points.

**Proposition 4.** If the DPN condition stands, we have the following decoupled expression for the posterior of each latent process:

$$p(\hat{u}_{i*}|\mathbf{Y}) = \mathcal{N}(\mathbf{k}_{i*}^T(\mathbf{K}_i + \sigma_i^2\mathbf{I}_n)^{-1}\mathbf{T}_i\mathbf{Y}, k_{i**} - \mathbf{k}_{i*}^T(\mathbf{K}_i + \sigma_i^2\mathbf{I}_n)^{-1}\mathbf{k}_{i*}) \quad (8)$$

with  $\Sigma_{\mathbf{P}} = (\mathbf{H}^T\Sigma^{-1}\mathbf{H})^{-1} = \text{Diag}(\sigma_i^2)_{1 \leq i \leq q}$  and  $\mathbf{T}_i$  the  $i$ -th row of  $\mathbf{T}$ .

This is the expression of a standard single-output gaussian process regression and can thus be computed with time complexity  $O(n^3)$  per latent process. It can also be seen easily from equation (7) that the likelihood factorizes over latent processes if and only if  $\mathcal{N}(\mathbf{T}\mathbf{Y}_j|\mathbf{U}_j, \Sigma_{\mathbf{P}})$  does, i.e if  $\Sigma_{\mathbf{P}}$  is diagonal.

### 3.4 Probabilistic interpretation

The fact that the quantities  $\Sigma_{\mathbf{P}}$  and  $\mathbf{T}\mathbf{Y}$  play such an important role in all expressions<sup>2</sup> hints that they have a probabilistic meaning. The next proposition gives such an interpretation, mostly restating results from Bruinsma (2020, [6]): all previous properties stem from the two facts that  $\mathbf{T}\mathbf{Y}$  is a sufficient statistic of the model for the variable  $\mathbf{U}$ , and  $\Sigma_{\mathbf{P}}$  is the noise matrix contracted by  $\mathbf{T}$ , i.e  $\Sigma_{\mathbf{P}} = \mathbf{T}\Sigma\mathbf{T}^T$ .

**Proposition 5.** •  $\mathbf{T}$  is a generalized inverse of  $\mathbf{H}$ :  $\mathbf{T}\mathbf{H} = \mathbf{I}_q$ . Therefore,  $\mathbf{H}\mathbf{T}$  is a projection.

- $\mathbf{T}\mathbf{Y}$  is a maximum likelihood estimator for  $\mathbf{U}$ :  $\mathbf{T}\mathbf{Y} = \arg \max_{\mathbf{U}} p(\mathbf{Y}|\mathbf{U})$ . It is an unbiased estimator:  $\mathbb{E}[\mathbf{T}\mathbf{Y}|\mathbf{U}] = \mathbf{U}$ .
- $\mathbf{T}\mathbf{Y}$  is a minimal sufficient statistic of the data  $\mathbf{Y}$  for the variable  $\mathbf{U}$ . In other words,  $\mathbf{T}\mathbf{Y}$  contains all the information required to compute the best possible estimate of  $\mathbf{U}$ . Consequently,  $p(\mathbf{U}|\mathbf{Y}) = p(\mathbf{U}|\mathbf{T}\mathbf{Y})$ .
- $\mathbf{T}\Sigma\mathbf{T}^T = \Sigma_{\mathbf{P}}$ , so that  $\mathbf{T}\mathbf{Y}|\mathbf{U} \sim \mathcal{N}(\mathbf{U}_{\mathbf{v}}, \Sigma_{\mathbf{P}} \otimes \mathbf{I}_n)$
- The latent processes of any LMC model are independent conditionally upon observations if and only if  $\Sigma_{\mathbf{P}}$  is diagonal.

## 4 The diagonally-projected noise condition

We have not given so far a complete procedure for optimizing the likelihood  $p(\mathbf{Y})$ , because this requires a proper joint parametrization of  $\mathbf{H}$  and  $\Sigma$ : these matrices are coupled by the DPN condition, so they cannot be optimized independently. Such a parametrization is provided in the next section.

### 4.1 Characterization of diagonally-projected noises

We have shown the DPN hypothesis 2 to be crucial to the efficient computation of the LMC, but we yet have to explain how to enforce it. Reminding that it is written ( $\mathbf{H}^T\Sigma^{-1}\mathbf{H}$  is diagonal), we hint that it can be expressed as some orthogonality condition between rows of  $\Sigma^{-1}$  and columns of  $\mathbf{H}$ . We therefore introduce the QR decomposition of  $\mathbf{H}$ :  $\mathbf{H} = \mathbf{Q}\mathbf{R}$ , where  $\mathbf{Q}$  has orthonormal columns and shape  $p \times q$ , and  $\mathbf{R}$  is upper-triangular of size  $q \times q$ . We also introduce  $\mathbf{Q}_{\perp}$ , a  $p \times (p - q)$  orthonormal complement of  $\mathbf{Q}$  which for now is arbitrary. We state the following lemma:

---

<sup>2</sup>Equation (3) can be rephrased as  $\mathbb{E}(\mathbf{U}_{\mathbf{v}}|\mathbf{Y}) = [\text{Diag}(\mathbf{K}_i^{-1}) + \Sigma_{\mathbf{P}}^{-1} \otimes \mathbf{I}_n]^{-1} \text{vec}(\mathbf{Y}\mathbf{T}^T\Sigma_{\mathbf{P}}^{-1})$ ,  $\mathbb{V}(\mathbf{U}_{\mathbf{v}}|\mathbf{Y}) = (\text{Diag}(\mathbf{K}_i^{-1}) + \Sigma_{\mathbf{P}}^{-1} \otimes \mathbf{I}_n)^{-1}$ .



**Lemma 1.** Any symmetric matrix  $\mathcal{S}$  can be decomposed as  $\mathcal{S} = \mathbf{Q}\mathbf{A}\mathbf{Q}^T + \mathbf{Q}_\perp\mathbf{B}\mathbf{Q}_\perp^T + \mathbf{Q}\mathbf{C}\mathbf{Q}_\perp^T + \mathbf{Q}_\perp\mathbf{C}^T\mathbf{Q}^T$ , with  $\mathbf{A}, \mathbf{B}$  symmetric matrices and  $\mathbf{C}$  a  $q \times (p - q)$  matrix.

A first characterization of the DNP condition follows:

**Proposition 6.** Let  $\Sigma^{-1} = \mathbf{Q}\mathbf{A}\mathbf{Q}^T + \mathbf{Q}_\perp\mathbf{B}\mathbf{Q}_\perp^T + \mathbf{Q}\mathbf{C}\mathbf{Q}_\perp^T + \mathbf{Q}_\perp\mathbf{C}^T\mathbf{Q}^T$  be a decomposition of  $\Sigma^{-1}$  as in lemma 1. Then  $\Sigma_{\mathbf{P}} = \mathbf{R}^{-1}\mathbf{A}^{-1}\mathbf{R}^{-T}$ , (where  $\mathbf{R}^{-T}$  denotes the inverse transpose of  $\mathbf{R}$ ) and the DPN condition is equivalent to  $(\mathbf{A} = \mathbf{R}^{-T}\mathbf{D}\mathbf{R}^{-1})$  for some diagonal matrix  $\mathbf{D}$  of size  $q$ .

**Remark 2.** Notice that  $\mathbf{A}, \mathbf{B}$  and  $\mathbf{C}$  are simply subblocks of  $\Sigma^{-1}$  in the basis spanned by  $\mathbf{Q}$  and  $\mathbf{Q}_\perp$ , and that  $\mathbf{B}$  and  $\mathbf{C}$  remain arbitrary: the DPN condition only involves a  $q \times q$  submatrix of  $\Sigma^{-1}$ , with  $q \ll p$  in most cases. This observation, which hints the benign nature of this assumption, is made more precise in Annex C, where a closed-form expression of the optimal  $\mathbf{D}$  and a noise correction procedure are provided.

Computations with the LMC involve  $\Sigma^{-1}$  but also  $\Sigma$ . We thus seek to express  $\Sigma^{-1}$  in a factorized rather than additive form.

**Proposition 7.** Given its decomposition 1, the following factorization stands for any symmetric matrix  $\Sigma^{-1}$ :

$$\Sigma^{-1} = \mathbf{Q}_+ \mathbf{R}_+^{-T} \mathbf{D}_+^{-1} \mathbf{R}_+^{-1} \mathbf{Q}_+^T, \quad (9)$$

where:  $\mathbf{Q}_+ = \begin{pmatrix} \mathbf{Q} & \mathbf{Q}_\perp \end{pmatrix}$ ,  $\mathbf{R}_+ = \begin{pmatrix} \mathbf{R} & \mathbf{0} \\ \mathbf{0} & \mathbf{I}_{p-q} \end{pmatrix}$ ,  $\mathbf{D}_+^{-1} = \begin{pmatrix} \mathbf{D} & \mathbf{M} \\ \mathbf{M}^T & \mathbf{B} \end{pmatrix}$ ,  $\mathbf{D} = \mathbf{R}^T \mathbf{A} \mathbf{R}$  and  $\mathbf{M} = \mathbf{R}^T \mathbf{C}$ . By construction  $\mathbf{Q}_+$  is a  $p \times p$  orthonormal matrix and  $\mathbf{R}_+$  is a  $p \times p$  upper triangular matrix. By prop.6,  $\mathbf{D} = \Sigma_{\mathbf{P}}^{-1}$ , so it is diagonal if and only if the DPN condition stands.

**Corollary 1.**

$$\Sigma = \mathbf{Q}_+ \mathbf{R}_+ \mathbf{D}_+ \mathbf{R}_+^T \mathbf{Q}_+^T, \quad (10)$$

where the blocks of  $\mathbf{D}_+$  are denoted  $\mathbf{D}_+ = \begin{pmatrix} \tilde{\mathbf{D}} & \tilde{\mathbf{M}} \\ \tilde{\mathbf{M}}^T & \tilde{\mathbf{B}} \end{pmatrix}$ , and can be computed from blockwise inversion formulas.

If we decompose  $\Sigma$  in the way of lemma 1, that is,  $\Sigma = \mathbf{Q}\tilde{\mathbf{A}}\mathbf{Q}^T + \mathbf{Q}_\perp\tilde{\mathbf{B}}\mathbf{Q}_\perp^T + \mathbf{Q}\tilde{\mathbf{C}}\mathbf{Q}_\perp^T + \mathbf{Q}_\perp\tilde{\mathbf{C}}^T\mathbf{Q}^T$ , noticing the formal analogy between the above factorization and this of  $\Sigma^{-1}$  (inverting  $\mathbf{R}$  and  $\mathbf{R}^{-T}$ ), we get from prop.7 that  $\tilde{\mathbf{D}} = \mathbf{R}^{-1}\tilde{\mathbf{A}}\mathbf{R}^{-T}$  and  $\tilde{\mathbf{M}} = \mathbf{R}^{-1}\tilde{\mathbf{C}}$ .

All this parametrization also yields valuable insight about the model. For instance, we have the following expressions for  $\mathbf{T}$ :

**Proposition 8.**

$$\mathbf{T} = \mathbf{H}^+ + \Sigma_{\mathbf{P}} \mathbf{H}^T \mathbf{Q} \mathbf{C} \mathbf{Q}_\perp^T \quad (11)$$

$$= \mathbf{H}^+ (\mathbf{I}_p - \Sigma \mathbf{Q}_\perp \tilde{\mathbf{B}}^{-1} \mathbf{Q}_\perp^T) \quad (12)$$

where  $\mathbf{H}^+$  is the Moore-Penrose pseudoinverse of  $\mathbf{H}$ . These expressions don't depend on a particular choice of the orthogonal complement  $\mathbf{Q}_\perp$ .

**Corollary 2.** If  $\mathbf{C} = \mathbf{U}^T \Sigma \mathbf{U}_\perp = \mathbf{0}$ , all expressions greatly simplify:  $\mathbf{T} = \mathbf{H}^+$ ,  $\mathbf{M} = \mathbf{0}$ ,  $\tilde{\mathbf{M}} = \mathbf{0}$ ,  $\tilde{\mathbf{D}} = \mathbf{D}^{-1}$ ,  $\tilde{\mathbf{B}} = \mathbf{B}^{-1}$ . We name this case the block-diagonal noise condition (BDN).

## 4.2 Optimization of the marginal log-likelihood

**Proposition 9.** Under the DPN condition, we have the following decoupled expression for the marginal log-likelihood:

$$\begin{aligned} -2 \log p(\mathbf{Y}) &= (p - q)n \log 2\pi + 2n \log |\mathbf{R}| + n \log |\tilde{\mathbf{B}}| \\ &\quad + \text{Tr}(\mathbf{Y}^T \mathbf{Q}_\perp \tilde{\mathbf{B}}^{-1} \mathbf{Q}_\perp^T \mathbf{Y}) + \sum_{i=1}^q \log \mathcal{N}(\mathbf{T}_i \mathbf{Y} | \mathbf{0}, \mathbf{K}_i + \sigma_i \mathbf{I}_n) \end{aligned} \quad (13)$$

$\tilde{\mathbf{B}}^{-1}$ ,  $\Sigma_{\mathbf{P}}$  and  $\mathbf{M}$  (present in this expression through  $\mathbf{T}$ ) form a full parametrization of the noise and can be optimized independently.



Notice that  $\mathbf{M}$  and  $\tilde{\mathbf{B}}$  are noise parameters, which are likely to be of low magnitude and low relevance to the model:  $\tilde{\mathbf{B}}$  can be seen as a "discarded noise" which is absent from the posteriors and acts on the likelihood essentially by interfering with  $\mathbf{Q}_\perp$ , while  $\mathbf{M}$  couples the projected noise with the discarded noise. We can therefore try to further simplify the model, for instance by setting  $\mathbf{M} = \mathbf{0}$  or assuming  $\tilde{\mathbf{B}}$  to be scalar or diagonal. In fact, the latter assumption is not even restrictive, as the following proposition shows:

**Proposition 10.** *The projection matrix  $\mathbf{T}$  and posteriors of the model don't depend on  $\tilde{\mathbf{B}}$ ; moreover,  $\tilde{\mathbf{B}}$  can be restricted to be diagonal without incidence on the likelihood.*

Even if the suggested simplifications had little impact on the values of estimators, they could modify the behavior of parameter optimization. One objective of the upcoming experimental section will be to assess which of them should be favored in practice.

Noting from prop.(11) that  $\mathbf{T} = \mathbf{R}^{-1}\mathbf{Q}^\mathbf{T} + \Sigma_\mathbf{P}\mathbf{M}\mathbf{Q}_\perp^\mathbf{T}$ , and setting  $\tilde{\mathbf{B}}^{-1} = \mathbf{L}\mathbf{L}^\mathbf{T}$  the Cholesky decomposition of  $\tilde{\mathbf{B}}^{-1}$ , we can finally select the following parameters for the model, which we from now on refer to as *projected LMC*:

- An orthonormal  $p \times p$  matrix  $\mathbf{Q}_+$  (joint optimization of  $\mathbf{Q}$  and  $\mathbf{Q}_\perp$ , which are orthogonal to each other). For a parametrization of orthonormal matrices, see for instance this of Lezcano-Casado (2019, [12]) implemented in Pytorch;
- An upper-triangular  $q \times q$  matrix  $\mathbf{R}$ ;
- A  $(p-q) \times (p-q)$  Cholesky factor  $\mathbf{L}$  which by prop.10 can be assumed diagonal, optimization considerations aside;
- A  $q \times (p-q)$  matrix  $\mathbf{M}$  with no specific property;
- A  $q \times q$  positive diagonal matrix  $\Sigma_\mathbf{P}$ , which is integrated to the parameters of the latent processes GPs ( $\sigma_i$ 's of prop. 4);
- All parameters of the latent kernels  $\mathbf{K}_i$ .

**Remark 3.** *The mixing matrix of the OILMM is written  $\mathbf{H} = \mathbf{Q}\mathbf{S}^{1/2}$  with  $\mathbf{Q}$  orthonormal and  $\mathbf{S}$  positive diagonal, and its noise model  $\Sigma = \sigma\mathbf{I} + \mathbf{H}\mathbf{D}\mathbf{H}^\mathbf{T}$  with  $\mathbf{D}$  diagonal. Rewriting the latter  $\Sigma = \mathbf{Q}_\perp(\sigma\mathbf{I})\mathbf{Q}_\perp^\mathbf{T} + \mathbf{Q}\mathbf{S}^{1/2}(\mathbf{D} + \sigma\mathbf{S}^{-1})\mathbf{S}^{1/2}\mathbf{Q}^\mathbf{T}$ , and identifying  $\mathbf{S}^{1/2} \equiv \mathbf{R}$ ,  $\mathbf{D} + \sigma\mathbf{S}^{-1} \equiv \tilde{\mathbf{D}}$  and  $\sigma\mathbf{I} \equiv \tilde{\mathbf{B}}$ , we see that the OILMM is a special case of our model, where  $\mathbf{R}$  is constrained to be positive diagonal instead of triangular,  $\mathbf{M}$  is zero and  $\tilde{\mathbf{B}}$  is scalar instead of diagonal. The restriction on  $\mathbf{R}$  is likely to be the most significant; we study the effect of these various simplifications in the next experimental section.*

## 5 Experimental results

### 5.1 Preparation of synthetic data

In this article, we restrict ourselves to testing on synthetic data<sup>3</sup>, in order to perform a parametric study on its properties. This data is generated according to a univariate LMC model: its latent processes are defined by  $N_{lat}$  1D Matern kernels ( $\nu = 2.5$ ) with lengthscales equidistant in the interval  $[l_{min}, l_{max}]$ , and sampled at the locations  $\mathbf{X}_{train}$  ( $N_{points}$  points equidistant in  $[-1, 1]$ ) and  $\mathbf{X}_{test}$  (500 points sampled uniformly in the same interval). The coefficients of the mixing matrix  $\mathbf{H}$  are sampled from independent normal distribution  $\mathcal{N}(0, 1)$ . After latent signals are mixed, structured noise is added in a manner inspired from Rakitsch (2013, [21]): a parameter  $\mu_{noise}$  controls the signal-to-noise proportion ( $Data_{full} = \mu_{noise} Data_{noise} + (1 - \mu_{noise}) Data_{signal}$ ), and another  $\mu_{struc}$  rules the proportion of structured-to-unstructured noise ( $Data_{noise} = \mu_{str} Noise_{str} + (1 - \mu_{str}) Noise_{ind}$ ).  $Noise_{str}$  is obtained by the mixing of  $N_{lat}^{noise}$  white noise processes by a matrix  $\mathbf{H}_{noise}$ , generated in the same way as  $\mathbf{H}$ , while  $Noise_{ind}$  is simply the concatenation of  $N_{tasks}$  independent white noises. The noise thus contains a part that is correlated over all tasks, and one that is specific to each task. Overall the synthetic data is described by 8 parameters; when they are not varied for an experiment or explicitly specified, their fixed values are the following:  $N_{tasks} = 10$ ,  $N_{lat} = 2$ ,  $N_{lat}^{noise} = 3$ ,  $N_{points} = 50$ ,  $\mu_{noise} = 0.05$ ,  $\mu_{str} = 0.5$ ,  $l_{min} = 0.1$  and  $l_{max} = 0.5$ . All tests are run  $N_{rep}$  times with data generated from as many random seeds, and results are averaged to attenuate the fluctuations caused by data randomness ( $N_{rep} = 10$  for graphs and 100 for tables).

<sup>3</sup>Tests have also been made with great success on real nuclear data for an application in neutronics; the results will be published in subsequent work.



## 5.2 Tested models

This parametric study has several goals, the main one being to **verify the good behavior of the projected model in various setups**. To this end, we compare it with the exact naive LMC (this of eq. (1)) and with a state-of-the-art variational LMC, suspecting that the naive model may have suboptimal performance due to impractical linear algebra (inversion of large ill-conditioned matrices, etc). This includes **assessing the effect of the DPN condition in situations of large and structured noise**, to determine whether projected LMC should be avoided in this case – or eventually corrected, such as suggested in Annex C. The last aim is to **test several possible implementations and simplifications of the model**, as mentioned in section 4.2. We therefore end up with 7 models to test: **exact** (naïve LMC with full  $np \times np$  covariance), **var** (variational LMC as described in Hensman (2015, [10]) and implemented in `gpytorch` (2018, [8]), with a Cholesky variational distribution and a number  $N_{points}/1.5$  of learned inducing points<sup>4</sup>), **proj** (fully parametrized projected LMC with dense matrix  $\tilde{\mathbf{B}}$ ), **diagproj** (projected LMC with diagonal  $\tilde{\mathbf{B}}$ ), **bdn** (projected LMC with  $\mathbf{M} = \mathbf{0}$ ), **bdn\_diag** (projected LMC with  $\mathbf{M} = \mathbf{0}$  and diagonal  $\tilde{\mathbf{B}}$ ) and **oilmm** (projected LMC with positive diagonal  $\mathbf{R}$ , scalar  $\tilde{\mathbf{B}}$  and  $\mathbf{M} = \mathbf{0}$ ). Both **exact** and **var** models are implemented with a fully general likelihood, putting no constraint on their  $\Sigma$  matrix. For all models, the chosen kernel types and number of latent processes are always this of the data (no model misspecification).

The training protocol for each model (optimizer, learning rate schedule, number of iterations, initialization, stopping criterion...) was hand-refined and finally taken identical for all of them, as the chosen common scheme yielded near-optimal convergence for all; it is specified in Annex D.

## 5.3 Results of the parametric study

**DPN condition severity.** The first and main observation is that *all projected models overall perform nearly as good as the state-of-the-art variational LMC*, and better than the naive exact implementation, even in setups where high-magnitude structured noise should handicap them. This way, figure 1 shows that for the highest noise magnitudes ( $\mu_{noise} = 0.5$ , corresponding to a signal-to-noise ratio of 1) and a highly-structured noise ( $\mu_{str} = 0.99$ ), the L1 test error of the projected model **diagproj** is as low as this of its exact and variational counterparts: in fact, all of them follow the expected asymptote  $Err_{L1} \simeq \mu_{noise}$ . Surprisingly, it is at lower noise magnitudes that the discrepancy is larger; this behavior also occurs for lower values of  $\mu_{str}$ .

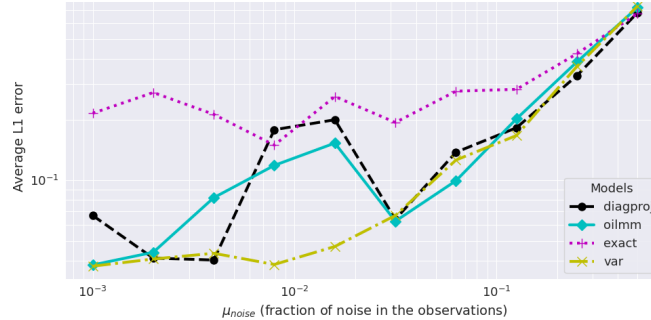


Figure 1: Average L1 error of several models for increasing data noise magnitude, with highly structured noise ( $\mu_{str} = 0.99$ )

Even more surprising, figure 2 which plots the L1 test error against  $\mu_{str}$  shows no sign of underperformance of the projected model for highly-structured noises (large  $\mu_{str}$ ), even though the noise has a large amplitude in this test ( $\mu_{noise} = 0.3$ ). Here again, the discrepancy is larger in the parameter region which is theoretically more favorable to the projected models (low  $\mu_{str}$ ), indicating that the occasional underperformance of projected models relative to the variational one must have other causes than the DPN condition – for instance a less favorable parametrization. These observations still stand for lower values of  $\mu_{noise}$ .

**Simplifications and parametrization of the projected LMC.** Figures 1 and 2 only display one projected model (**diagproj**) for clarity, because it is this of greatest interest being the no-approximation model with fewest parameters, and because the plots of all projected models are very similar. We nonetheless wish to assess the merits of the various contemplated implementations. It happens that **simplifications of the projected LMC have little impact on prediction accuracy, but larger effects on other quantities**. In table 1 we compare all 7 models on  $N_{rep} = 100$  random realizations of a challenging setup<sup>5</sup>:  $\mu_{noise} = 0.25$ ,  $\mu_{str} = 0.5$ . The

<sup>4</sup>Picking a larger number of learned inducing points or even choosing frozen inducing points at all observed locations, although theoretically more accurate, proved less stable in practice.

<sup>5</sup>But not the most challenging possible: as it can be seen on figures 1 and 2, the hardest setups tend to "squash" models near one another, all behaving equally poorly.



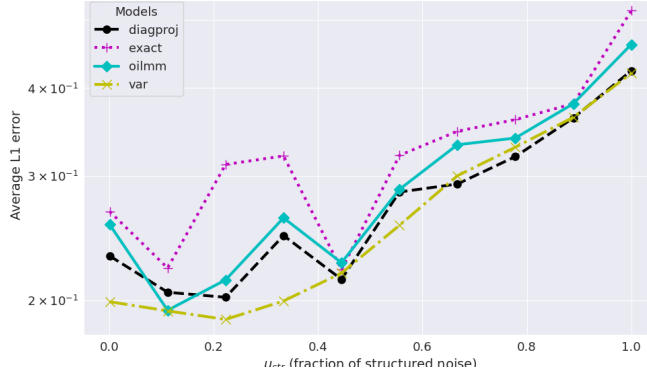


Figure 2: Average L1 error of several models for increasing proportion of structured noise, with large noise magnitude ( $\mu_{noise} = 0.3$ )

performance metrics are: the number of optimizer iterations until convergence  $N_{iter}$ , the training time  $t_{train}$  (in seconds), the average L1 error  $Err_{L1}$ , the 95% quantile of L1 errors  $Q_{L1}^{95}$ , the Predictive Variance Adequacy ( $PVA = \log \left( \frac{1}{N_{points}} \frac{1}{N_{tasks}} \sum_{i=1}^{N_{points}} \sum_{j=1}^{N_{tasks}} \frac{(y_{ij} - \hat{y}_{ij})^2}{\hat{v}_{ij}} \right)$ , with  $y_{ij}$  the true value of output  $j$  at point  $i$ ,  $\hat{y}_{ij}$  the corresponding estimated value and  $\hat{v}_{ij}$  the corresponding predicted variance) which assesses whether the predictive distribution has the right width, and the mixing matrix correctness  $H_{corr}$  defined as the correlation between true and estimated mixing matrices<sup>6</sup>. One can see that convergence speed is especially affected by simplifications: while the BDN assumption ( $\mathbf{M} = \mathbf{0}$ , see prop. 2) enforced by the **bdn**, **bdn\_diag** and **oilmm** models doesn't seem to accelerate optimization much, enforcing  $\tilde{\mathbf{B}}$  to be diagonal (which is the case of **diagproj**, **bdn\_diag** and **oilmm**) dramatically does. Overall, all models exhibit very similar performances – except for the training duration – but the naive exact LMC **exact**, which is probably hindered by its poor linear algebra.

Table 1: Performances of all models on a challenging case ( $\mu_{noise} = 0.25$ ,  $\mu_{str} = 0.5$ )

Model	$N_{iter}$	$t_{train}$	$Err_{L1}$	$Q_{L1}^{95}$	$PVA$	$H_{corr}$
var	1927	11	0.202	0.53	0.08	0.94
proj	4722	21	0.204	0.54	0.04	0.89
diagproj	1852	8	0.216	0.58	-0.14	0.87
bdn	4612	16	0.217	0.58	0.03	0.86
bdn_diag	1451	5	0.221	0.59	-0.03	0.86
oilmm	1131	4	0.233	0.63	-0.13	0.86
exact	1183	41	0.277	0.77	-1.26	0.84

Table 1 also shows that simplifications significantly impact the PVA. The desired value is  $PVA = 0$ , in which case the predicted variance exactly matches the squared observed error everywhere. The DPN assumption seems to lower it slightly, while the diagonal- $\tilde{\mathbf{B}}$  parametrization lowers it a lot more; however, it is not clear which prediction is better in general, as the ranking from this table contradicts this of following figure 3. Further experimentation and practice is thus required. It is useful to investigate the behavior of the PVA when varying data noise parameters: this is done in fig. 3 for  $\mu_{str}$ , with large noise magnitude  $\mu_{noise} = 0.3$ . The plots clearly show that for all projected models and unlike the variational one, noise complexity affects the quality of variance prediction; but also that this effect depends on the enforced simplifications. Model **bdn\_diag** appears to be the most robust in both table 1 and fig. 3, but has slightly larger prediction errors in general; a tradeoff could be made in this way depending on applications.

**Advantage over the OILMM.** A last simplification to investigate is the enforcement of a diagonal matrix  $\mathbf{R}$  (from the QR decomposition of  $\mathbf{H}$ ), only applied by the OILMM. This is probably the strongest approximation of all, as it involves the mixing matrix instead of little-important noise parameters; yet it appeared so far to have little effect on performance. This may be due to the way the mixing matrix of the data is generated: though it was designed to be "fully general" (all of its coefficients are sampled from i.i.d normal distributions),

<sup>6</sup>Minding the indeterminacy of the row sign and order.



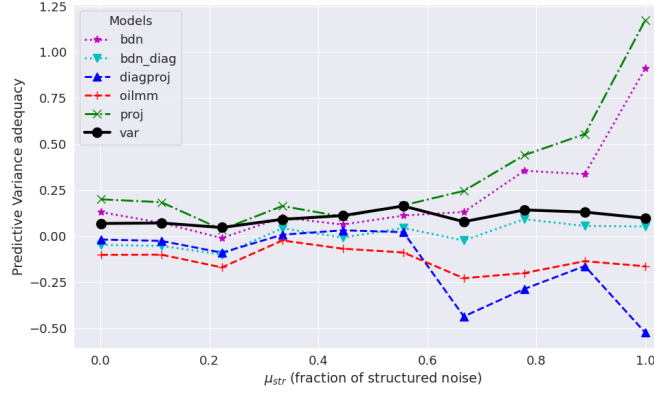


Figure 3: Average Predictive Variance Adequacy of several models for increasing proportion of structured noise, with large noise magnitude ( $\mu_{noise} = 0.3$ )

the large value of  $H_{corr}$  for the OILMM in table 1 hints that this scheme tends to produce matrices well-suited to this approximation. It can therefore be tried to experiment on more structured  $\mathbf{H}$  matrices, while keeping to "realistic" setups (configurations mimicking real-life data rather than artificially exploiting the weak spots of the OILMM). We designed such a mechanism, fully described in Annex E, making  $\mathbf{H}$  represent the intensity of wave signals with  $1/r^2$  amplitude decay, emitted from  $N_{lat}$  randomly-located sources and reaching  $N_{tasks}$  aligned and equidistant sensors. Contrary to the previous case, the OILMM – and this model only – then showed to be very sensitive to the number of latent processes, as displayed in figure 4. Its behavior even appears as pathological with errors of hundreds of percents, so it cannot be ruled out that different parametrization or optimization might improve it<sup>7</sup>. In any case, this constitutes a frailty which should be minded in applications, qualifying projected LMC as an alternative to OILMM, presumably more robust in setups where outputs are correlated by structure-rich mechanisms.

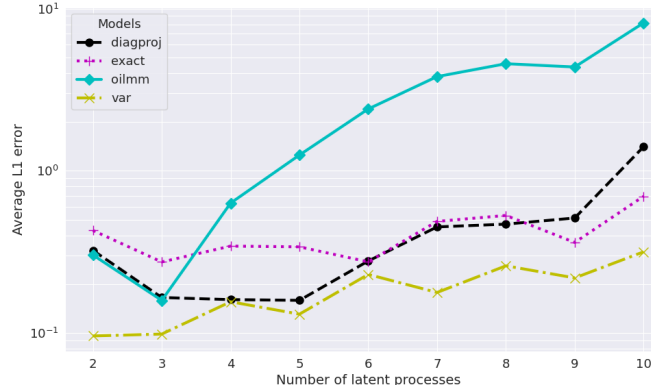


Figure 4: Average L1 error of several models for increasing number of latent functions (and  $N_{tasks} = 10$ ), with a "realistic" mixing matrix  $\mathbf{H}$  mimicking wave signal intensity from randomly-dispatched sources to aligned sensors, and low noise ( $\mu_{noise} = 0.05$ ).

**Other observations.** More experiments varying the remaining data parameters were carried out, but revealed few additional phenomena. Increasing the complexity of structured noise through its rank  $N_{lat}^{noise}$  yields plots very similar to figures 2 and 3: large and heavily-structured noise doesn't affect the prediction accuracy of projected models more than this of non-projected ones, but deteriorates their predictive variance adequacy, some submodels being more robust against this effect (in particular **bdn\_diag** and **oilmm**). In the case of the realistic structured mixing matrix of the previous paragraph, increasing the number of tasks away from this of latent processes has an effect on the OILMM similar to increasing the latter towards the former like in fig.4. Otherwise, altering the other data parameters (modifying the number of training points, reducing the range of kernel lengthscales...) offered very little discriminative power over all models.

<sup>7</sup>Yet the stopping criterion (see Annex D) was met ahead of the maximal iterations budget.



## 6 Conclusion

In this article, we showed that the equations of the Linear Model of Co-regionalization could be reformulated in a way that reveals its low-rank latent structure. These expressions have the striking property – first observed by Bruinsma (2020, [6]) – of decoupling if and only if a certain condition on the noise is verified, enabling computation to be linear in the number of latent processes rather than cubic in the number of tasks. We gave a general parametrization of LMC models enforcing this noise assumption and optimized the marginal likelihood accordingly. We performed a parametric study on synthetic data, comparing several possible implementations of our resulting *projected LMC* between them and with concurrent approaches. Projected models showed to compete very well with state-of-the-art variational LMC, even in setups where they should theoretically be challenged (large and highly-structured noises). The various suggested implementation options had little effect on prediction accuracy, but greater impact on other quantities, such as optimization dynamics or predictive variance quality. We also exhibited a realistic configuration in which the projected LMC greatly benefits from its extended generality compared with the OILMM of Bruinsma.

In addition to yielding theoretical insights (see for instance Annex F for a comparison of the approximations made by several LMC models), the projected LMC appears as a viable and more straightforward alternative to its variational counterparts, in particular in applications where the inducing points approximation enforced by the latter is not desired. It can be implemented as a mere overlay of a batch single-output GP, by parametrizing a mixing matrix and adding a few simple extra terms to the likelihood. Its exact GP treatment also authorizes operations which are more cumbersome with variational methods, such as leave-one-out error computation (Rasmussen, 2006, [22]) and incorporation of new observations, (Jiang, 2020, [11]), ultimately facilitating the use of gaussian processes for multitask optimization and adaptive sampling.

## References

- M. A. Alvarez, L. Rosasco, and N. D. Lawrence (2012). *Kernels for Vector-Valued Functions: a Review*. Publisher: Now Foundations and Trends.
- I. Bilonis, N. Zabaras, B. A. Konomi, and G. Lin (2013). Multi-output separable Gaussian process: Towards an efficient, fully Bayesian paradigm for uncertainty quantification. *Journal of Computational Physics*, 241:212–239.
- C. M. Bishop (2006). *Pattern recognition and machine learning*. Publisher: Springer, Information science and statistics.
- E. Bonilla, K. Chian, and C. Williams (2007). Multi-task Gaussian Process Prediction. *Advances in Neural Information Processing Systems 20 (NIPS 2007)*.
- E. Bonilla, K. Krauth, and A. Dezfouli (2019). Generic Inference in Latent Gaussian Process Models. *Journal of Machine Learning Research* 20, 1–63.
- W. P. Bruinsma and al (2020). Scalable Exact Inference in Multi-Output Gaussian Processes. *ICML’20: Proceedings of the 37th International Conference on Machine Learning*.
- A. Dahl and E. Bonilla (2019). Grouped Gaussian processes for solar power prediction. *Machine Learning*, 108:1287–1306.
- J. Gardner and al (2018). **GPpyTorch**: Blackbox Matrix-Matrix Gaussian Process Inference with GPU Acceleration. *NIPS’18: Proceedings of the 32nd International Conference on Neural Information Processing Systems*, 7587–7597.
- M. Gu and W. Shen (2021). Generalized probabilistic principal component analysis of correlated data. *Journal of Machine Learning Research*, 21(13):1–41.
- J. Hensman and Z. Ghahramani (2015). Scalable Variational Gaussian Process Classification. *Proceedings of the 18th International Conference on Artificial Intelligence and Statistics (AISTATS)*, 38:351–360.
- S. Jiang and al (2020). Efficient Nonmyopic Bayesian Optimization via One-Shot Multi-Step Trees. *NIPS’20: Proceedings of the 34th International Conference on Neural Information Processing Systems*, 18039–18049.
- M. Lezcano-Casado (2019). Trivializations for Gradient-Based Optimization on Manifolds. *33rd Conference on Neural Information Processing Systems (NeurIPS 2019)*, 9154–9164



- H. Liu and al (2023). Learning Multitask Gaussian Process Over Heterogeneous Input Domains. *IEEE Transactions on Systems, Man, and Cybernetics: Systems*, Volume 53, Issue 10, 6232–6244
- H. Liu and al (2022). Scalable multi-task Gaussian processes with neural embedding of coregionalization. *Knowledge-Based Systems*, 247 (2022) 108775
- H. Liu, J. Cai, and Y. Ong (2018). Remarks on multi-output Gaussian process regression. *Knowledge-Based Systems*, 144:102–121.
- I. Loshchilov and F. Hutter (2019). Decoupled Weight Decay Regularization. *International Conference on Learning Representations*.
- W. J. Maddox, M. Balandat, A. G. Wilson, and E. Bakshy (2021). Bayesian Optimization with High-Dimensional Outputs. *Advances in Neural Information Processing Systems (NeurIPS 2021)*, 34:19274–19287.
- T. V. Nguyen and E. Bonilla (2014). Collaborative Multi-output Gaussian Processes. *UAI’14: Proceedings of the Thirtieth Conference on Uncertainty in Artificial Intelligence*, 643–652.
- A. Paszke and al (2019). PyTorch: An Imperative Style, High-Performance Deep Learning Library. *Advances in Neural Information Processing Systems 32*, 8024–8035.
- K. B. Petersen and M. S. Pedersen (2012). The Matrix Cookbook. [ <http://matrixcookbook.com> ]; Version: November 15, 2012.
- B. Rakitsch, C. Lippert, K. Borgwardt, and O. Stegle (2013). It is all in the noise: Efficient multi-task Gaussian process inference with structured residuals. *Advances in Neural Information Processing Systems 26 (NIPS 2013)*.
- C. E. Rasmussen and C. K. I. Williams (2006). Gaussian Processes for Machine Learning. Publisher: The MIT Press, ISBN 0-262-18253-X.
- Z. Tang, S. Li, K. S. Kim, and J. Smith (2022). Multi-Output Gaussian Process-Based Data Augmentation for Multi Building and Multi-Floor Indoor Localization. *WS22 IEEE ICC 2022 the 4th International Workshop on Data Driven Intelligence for Networks and Systems*.
- Y. W. Teh, M. Seeger, and M. I. Jordan (2005). Semiparametric latent factor models. *Proceedings of Machine Learning Research*, R5:333–340.
- Y. Wen and al (2021). Modeling and Analysis of Permanent Magnet Spherical Motors by a Multitask Gaussian Process Method and Finite Element Method for Output Torque. *IEEE Transactions on industrial electronics*, vol.68, no.9, 8540–8549.
- R. Zhang and X. Zhao (2020). Inverse Method of Centrifugal Pump Blade Based on Gaussian Process Regression. *Mathematical Problems in Engineering*, 2020(1):1–10.



## Appendix A CODE

Code available at <https://github.com/QWERTY6191/projected-lmc>

## Appendix B MISSING PROOFS

### B.1 Preliminary considerations

**Notation.** We adopt the following standard notation for any matrix  $\mathbf{M}$ :  $\mathbf{Sym}(\mathbf{M}) = \frac{\mathbf{M} + \mathbf{M}^T}{2}$ .

**Kronecker product manipulation.** We recall elementary properties of the Kronecker product :

$$(\mathbf{A} \otimes \mathbf{B})(\mathbf{C} \otimes \mathbf{D}) = (\mathbf{AC} \otimes \mathbf{BD}) \quad \text{for all matrices } \mathbf{A}, \mathbf{B}, \mathbf{C}, \mathbf{D} \text{ for which the products are defined ;} \quad (14)$$

$$(\mathbf{C}^T \otimes \mathbf{A})\text{vec}(\mathbf{B}) = \text{vec}(\mathbf{ABC}) \quad (15)$$

$$(\mathbf{A} \otimes \mathbf{B})^{-1} = \mathbf{A}^{-1} \otimes \mathbf{B}^{-1} \quad (\text{the inverse exists if and only if } \mathbf{A}^{-1}, \mathbf{B}^{-1} \text{ exist}) \quad (16)$$

**An identity on gaussian processes.**

**Lemma 2.**

$$\mathbb{E}_{U|Y} [\mathbb{E}_{u^*}(\mathbf{u}^* | \mathbf{Y}, \mathbf{U})] = \text{Diag}(\mathbf{k}_{i*}^T) \text{Diag}(\mathbf{K}_i^{-1}) \mathbb{E}_{U|Y}(\mathbf{U}_v | \mathbf{Y}) \quad (17)$$

*Proof.*

$$\begin{aligned} \mathbb{E}_{U|Y} [\mathbb{E}_{u^*}(\mathbf{u}^* | \mathbf{Y}, \mathbf{U})] &= \int \mathbb{E}_{u^*}(\mathbf{u}^* | \mathbf{Y}, \mathbf{U}) p(\mathbf{U} | \mathbf{Y}) d\mathbf{U} \\ &= \int \text{Diag}(\mathbf{k}_{i*}^T) \text{Diag}(\mathbf{K}_i^{-1}) \mathbf{U}_v p(\mathbf{U} | \mathbf{Y}) d\mathbf{U} \\ &= \text{Diag}(\mathbf{k}_{i*}^T) \text{Diag}(\mathbf{K}_i^{-1}) \mathbb{E}_{U|Y}(\mathbf{U}_v | \mathbf{Y}) \end{aligned}$$

The second equality holds by the conditioning property of GPs, and because  $\mathbb{E}_{u^*}(\mathbf{u}^* | \mathbf{Y}, \mathbf{U})$  doesn't depend on  $\mathbf{Y}$  (conditionnally on their corresponding latent values, observed values of a GP are independent of all other variables of the model).  $\square$

**A useful matrix identity.**

**Lemma 3.** For all invertible matrices  $\mathbf{A}, \mathbf{B}$  and all matrix  $\mathbf{C}$  conformable with them,  $\mathbf{C}^T(\mathbf{CAC}^T + \mathbf{B})^{-1}\mathbf{C} = (\mathbf{A} + \mathbf{C}^T\mathbf{BC})^{-1}$ . Note that  $\mathbf{A}$  and  $\mathbf{B}$  are not necessarily of the same size, so  $\mathbf{C}$  can be rectangular.

*Proof.*

$$\begin{aligned} \mathbf{C}^T(\mathbf{CAC}^T + \mathbf{B})^{-1}\mathbf{C} &= \mathbf{A}^{-1} (\mathbf{AC}^T(\mathbf{CAC}^T + \mathbf{B})^{-1}\mathbf{CA}) \mathbf{A}^{-1} \\ &= \mathbf{A}^{-1} (\mathbf{AC}^T(\mathbf{CAC}^T + \mathbf{B})^{-1}\mathbf{CA} - \mathbf{A}) \mathbf{A}^{-1} + \mathbf{A}^{-1} \\ &= \mathbf{A}^{-1} - (\mathbf{A}^{-1} + \mathbf{C}^T\mathbf{BC})^{-1} \mathbf{A}^{-1} + \mathbf{A}^{-1} \quad \text{by backward Woodbury's identity} \\ &= (\mathbf{A} + \mathbf{C}^T\mathbf{BC})^{-1} \quad \text{again by backward Woodbury's identity.} \end{aligned}$$

$\square$

### B.2 Proof of prop.1

**Proposition 1.**

$$p(\mathbf{U}_v | \mathbf{Y}) = \mathcal{N} \left( [\text{Diag}(\mathbf{K}_i^{-1}) + \mathbf{H}^T \Sigma^{-1} \mathbf{H} \otimes \mathbf{I}_n]^{-1} \text{vec}(\mathbf{Y}^T \Sigma^{-1} \mathbf{H}), [\text{Diag}(\mathbf{K}_i^{-1}) + \mathbf{H}^T \Sigma^{-1} \mathbf{H} \otimes \mathbf{I}_n]^{-1} \right) \quad (18)$$



*Proof.* All involved variables being jointly gaussian, we know that  $p(\mathbf{U}|\mathbf{Y})$  is gaussian ; it suffices to find its mean and variance. By Baye's rule,  $p(\mathbf{U}|\mathbf{Y}) \propto p(\mathbf{Y}|\mathbf{U})p(\mathbf{U})$ , the proportionality constant being the likelihood  $p(\mathbf{Y})$  which is independant of the latent variables  $\mathbf{U}$ . By definition of the model, we have (using the symmetry of  $\Sigma$  in the second equality):

$$\begin{aligned} p(\mathbf{Y}|\mathbf{U})p(\mathbf{U}) &\propto \exp\left\{-\frac{1}{2}(\mathbf{Y}_v - (\mathbf{H} \otimes \mathbf{I}_n)\mathbf{U}_v)^T (\Sigma^{-1} \otimes \mathbf{I}_n) (\mathbf{Y}_v - (\mathbf{H} \otimes \mathbf{I}_n)\mathbf{U}_v) - \frac{1}{2}\mathbf{U}_v^T \text{Diag}(\mathbf{K}_i^{-1})\mathbf{U}_v\right\} \\ &\propto \exp\left\{-\frac{1}{2}\mathbf{Y}_v^T (\Sigma^{-1} \otimes \mathbf{I}_n)\mathbf{Y}_v - 2\mathbf{U}_v^T (\mathbf{H}^T \Sigma^{-1} \otimes \mathbf{I}_n)\mathbf{Y}_v + \mathbf{U}_v^T (\text{Diag}(\mathbf{K}_i^{-1}) + \mathbf{H}^T \Sigma^{-1} \mathbf{H} \otimes \mathbf{I}_n)\mathbf{U}_v\right\} \end{aligned}$$

On the other hand,  $p(\mathbf{Y}|\mathbf{U})p(\mathbf{U})$  being gaussian, there exists a covariance matrix  $\tilde{\mathbf{K}}$  and a mean vector  $\hat{\mathbf{U}}_v$  such that :

$$\begin{aligned} p(\mathbf{Y}|\mathbf{U})p(\mathbf{U}) &\propto \exp\left\{-\frac{1}{2}(\mathbf{U}_v - \hat{\mathbf{U}}_v)^T \tilde{\mathbf{K}}^{-1} (\mathbf{U}_v - \hat{\mathbf{U}}_v)\right\} \\ &= \exp\left\{-\frac{1}{2}\mathbf{U}_v^T \tilde{\mathbf{K}}^{-1} \mathbf{U}_v - 2\mathbf{U}_v^T \tilde{\mathbf{K}}^{-1} \hat{\mathbf{U}}_v + \hat{\mathbf{U}}_v^T \tilde{\mathbf{K}}^{-1} \hat{\mathbf{U}}_v\right\} \end{aligned}$$

Therefore, to compute  $\tilde{\mathbf{K}}$  and  $\hat{\mathbf{U}}$ , one simply has to identify the terms in  $\mathbf{U}$  between the above expressions, as all the terms which don't depend on  $\mathbf{U}$  are compensated by the likelihood (denominator of Baye's formula). Proceeding as such, we obtain :

$$\begin{cases} \tilde{\mathbf{K}}^{-1} &= \text{Diag}(\mathbf{K}_i^{-1}) + \mathbf{H}^T \Sigma^{-1} \mathbf{H} \otimes \mathbf{I}_n \\ \tilde{\mathbf{K}}^{-1} \hat{\mathbf{U}}_v &= (\mathbf{H}^T \Sigma^{-1} \otimes \mathbf{I}_n) \mathbf{Y}_v = \text{vec}(\mathbf{Y}^T \Sigma^{-1} \mathbf{H}) \end{cases}$$

By definition,  $\hat{\mathbf{U}}_v$  is the mean vector of  $p(\mathbf{U}_v|\mathbf{Y})$  and  $\tilde{\mathbf{K}}$  is its covariance matrix, hence the result.  $\square$

### B.3 Proof of prop.2

**Proposition 2.**

$$\begin{aligned} \mathbb{E}(\hat{\mathbf{u}}_*|\mathbf{Y}) &= \text{Diag}(\mathbf{k}_{i*}) [\text{Diag}(\mathbf{K}_i) + (\mathbf{H}^T \Sigma^{-1} \mathbf{H})^{-1} \otimes \mathbf{I}_n]^{-1} \text{vec}(\mathbf{Y}^T \Sigma^{-1} \mathbf{H} (\mathbf{H}^T \Sigma^{-1} \mathbf{H})^{-1}) \\ \mathbb{V}(\hat{\mathbf{u}}_*|\mathbf{Y}) &= \text{Diag}(k_{i**}) - \text{Diag}(\mathbf{k}_{i*}^T) [\text{Diag}(\mathbf{K}_i) + (\mathbf{H}^T \Sigma^{-1} \mathbf{H})^{-1} \otimes \mathbf{I}_n]^{-1} \text{Diag}(\mathbf{k}_{i*}) \end{aligned}$$

*Proof.* We start with the estimated variance. By hypothesis of the model, the  $u_i$ 's follow GPs of kernels  $k_i$ 's, so we have by lemma 2:

$$\begin{aligned} \mathbb{E}(\hat{\mathbf{u}}_*|\mathbf{Y}) &= \text{Diag}(\mathbf{k}_{i*}^T) \text{Diag}(\mathbf{K}_i^{-1}) \mathbb{E}(\mathbf{U}_v|\mathbf{Y}) \\ &= \text{Diag}(\mathbf{k}_{i*}^T) \text{Diag}(\mathbf{K}_i^{-1}) [\text{Diag}(\mathbf{K}_i^{-1}) + \mathbf{H}^T \Sigma^{-1} \mathbf{H} \otimes \mathbf{I}_n]^{-1} (\mathbf{H}^T \Sigma^{-1} \otimes \mathbf{I}_n) \mathbf{Y}_v \\ &= \text{Diag}(\mathbf{k}_{i*}^T) [\text{Diag}(\mathbf{K}_i) + (\mathbf{H}^T \Sigma^{-1} \mathbf{H})^{-1} \otimes \mathbf{I}_n]^{-1} ((\mathbf{H}^T \Sigma^{-1} \mathbf{H})^{-1} \otimes \mathbf{I}_n) (\mathbf{H}^T \Sigma^{-1} \otimes \mathbf{I}_n) \mathbf{Y}_v \\ &= \text{Diag}(\mathbf{k}_{i*}^T) [\text{Diag}(\mathbf{K}_i) + (\mathbf{H}^T \Sigma^{-1} \mathbf{H})^{-1} \otimes \mathbf{I}_n]^{-1} \text{vec}(\mathbf{Y}^T \Sigma^{-1} \mathbf{H} (\mathbf{H}^T \Sigma^{-1} \mathbf{H})^{-1}) \end{aligned}$$

where the second equality is from prop.1, the third one from the matrix equality  $\mathbf{A}^{-1}(\mathbf{A}^{-1} + \mathbf{B}^{-1})^{-1} = (\mathbf{A} + \mathbf{B})^{-1} \mathbf{B}$  and the fourth one from basic facts 14 and 15.

We now compute the estimated variance from the law of total variance, conditioning on  $\mathbf{U}$ :  $\mathbb{V}(\hat{\mathbf{u}}_*|\mathbf{Y}) = \mathbb{E}_{U|\mathbf{Y}} [\mathbb{V}(\hat{\mathbf{u}}_*|\mathbf{Y}, \mathbf{U})] + \mathbb{V}_{U|\mathbf{Y}} [\mathbb{E}(\hat{\mathbf{u}}_*|\mathbf{Y}, \mathbf{U})]$ , where the subscript  $U|\mathbf{Y}$  means that  $\mathbb{E}_{U|\mathbf{Y}}(f(\mathbf{U})) = \int f(\mathbf{U}) p(\mathbf{U}|\mathbf{Y}) d\mathbf{U}$ . From there, we omit this subscript and treat each term separately. We also recall that  $p(\mathbf{u}^*|\mathbf{Y}, \mathbf{U})$  doesn't depend on  $\mathbf{Y}$  (conditionnally on their corresponding latent values, observed values of a GP are independent on all other variables of the model, and therefore  $\mathbb{E}_{u^*}(\mathbf{u}^*|\mathbf{Y}, \mathbf{U})$  doesn't depend on  $\mathbf{Y}$  (idem for the variance). It comes :

$$\begin{aligned} \mathbb{E}[\mathbb{V}(\hat{\mathbf{u}}_*|\mathbf{Y}, \mathbf{U})] &= \mathbb{E}[\text{Diag}(k_{i**}) - \text{Diag}(\mathbf{k}_{i*}^T) \text{Diag}(\mathbf{K}_i^{-1}) \text{Diag}(\mathbf{k}_{i*})] \\ &= (\text{Diag}(k_{i**}) - \text{Diag}(\mathbf{k}_{i*}^T) \text{Diag}(\mathbf{K}_i^{-1}) \text{Diag}(\mathbf{k}_{i*})) \end{aligned}$$

where the second equality holds because the term inside the expectation is deterministic. For the second term, we have :

$$\begin{aligned} \mathbb{V}_{U|\mathbf{Y}} [\mathbb{E}(\hat{\mathbf{u}}_*|\mathbf{Y}, \mathbf{U})] &= \mathbb{E}_{U|\mathbf{Y}} [\mathbb{E}((\hat{\mathbf{u}}_*|\mathbf{Y}, \mathbf{U})^2)] - \mathbb{E}_{U|\mathbf{Y}} [\mathbb{E}((\hat{\mathbf{u}}_*|\mathbf{Y}, \mathbf{U}))]^2 \\ &= \text{Diag}(\mathbf{k}_{i*}^T) \text{Diag}(\mathbf{K}_i^{-1}) \mathbb{E}(\mathbf{U}_v^2|\mathbf{Y}) \text{Diag}(\mathbf{K}_i^{-1}) \text{Diag}(\mathbf{k}_{i*}) - \text{Diag}(\mathbf{k}_{i*}^T) \text{Diag}(\mathbf{K}_i^{-1}) \mathbb{E}(\mathbf{U}_v|\mathbf{Y})^2 \text{Diag}(\mathbf{K}_i^{-1}) \text{Diag}(\mathbf{k}_{i*}) \\ &= \text{Diag}(\mathbf{k}_{i*}^T) \text{Diag}(\mathbf{K}_i^{-1}) \mathbb{V}(\mathbf{U}_v|\mathbf{Y}) \text{Diag}(\mathbf{K}_i^{-1}) \text{Diag}(\mathbf{k}_{i*}) \\ &= \text{Diag}(\mathbf{k}_{i*}^T) \text{Diag}(\mathbf{K}_i^{-1}) [\text{Diag}(\mathbf{K}_i^{-1}) + \mathbf{H}^T \Sigma^{-1} \mathbf{H} \otimes \mathbf{I}_n]^{-1} \text{Diag}(\mathbf{K}_i^{-1}) \text{Diag}(\mathbf{k}_{i*}) \end{aligned}$$



where the second equality stems from a relation analog to this of lemma 2, and the fourth is from prop.1.

Combining the two terms, it comes :  $\mathbb{V}(\hat{\mathbf{u}}_*|\mathbf{Y})$

$$\begin{aligned} &= \mathbf{Diag}(k_{i**}) - \mathbf{Diag}(\mathbf{k}_{i*}^T) \left[ \mathbf{Diag}(\mathbf{K}_i^{-1}) - \mathbf{Diag}(\mathbf{K}_i^{-1}) (\mathbf{Diag}(\mathbf{K}_i^{-1}) + \mathbf{H}^T \boldsymbol{\Sigma}^{-1} \mathbf{H} \otimes \mathbf{I}_n)^{-1} \mathbf{Diag}(\mathbf{K}_i^{-1}) \right] \mathbf{Diag}(\mathbf{k}_{i*}) \\ &= \mathbf{Diag}(k_{i**}) - \mathbf{Diag}(\mathbf{k}_{i*}^T) \left[ \mathbf{Diag}(\mathbf{K}_i) + (\mathbf{H}^T \boldsymbol{\Sigma}^{-1} \mathbf{H})^{-1} \otimes \mathbf{I}_n \right]^{-1} \mathbf{Diag}(\mathbf{k}_{i*}) \end{aligned}$$

where the second equality is from the Woodbury-type identity  $\mathbf{A}^{-1} - \mathbf{A}^{-1}(\mathbf{A}^{-1} + \mathbf{B}^{-1})^{-1} \mathbf{A}^{-1} = (\mathbf{A} + \mathbf{B})^{-1}$ .  $\square$

## B.4 Matricial proof of prop.2

We here give another proof of prop.2, which starts from the naive expression of LMC posteriors and uses only matrix algebra. It is a good example of involved manipulations of Kronecker products.

*Proof.* We start with the "naive" expression of the LMC estimators, as stated in section 1:

$$\mathbb{E}(\hat{\mathbf{y}}_*|\mathbf{Y}) = \mathbf{k}_*^T \mathcal{K}^{-1} \mathbf{Y}_v \quad (19)$$

$$\mathbb{V}(\hat{\mathbf{y}}_*|\mathbf{Y}) = \mathbf{k}_{**} - \mathbf{k}_*^T \mathcal{K}^{-1} \mathbf{k}_* \quad (20)$$

where the kernel considered here is the matricial kernel of the vector-valued GP:  $\mathbf{k}(\mathbf{x}, \mathbf{x}') = \sum_{i=1}^q \mathbf{B}_i k_i(\mathbf{x}, \mathbf{x}')$ , and we recall that  $\mathbf{K} = (\mathbf{H} \otimes \mathbf{I}_n) \mathbf{Diag}(\mathbf{K}_i) (\mathbf{H}^T \otimes \mathbf{I}_n)^8$ . Similarly, we have  $\mathbf{k}_* = (\mathbf{H} \otimes \mathbf{I}_n) \mathbf{Diag}(\mathbf{k}_i) \mathbf{H}^T$ , and  $\mathbf{k}_{**} = \mathbf{H} \mathbf{Diag}(\mathbf{k}_{i**}) \mathbf{H}^T$ . Anticipating on the cumbersome writing of Kronecker products, we adopt the following convention : for any matrix  $\mathbf{M}$ ,  $\tilde{\mathbf{M}} \equiv \mathbf{M} \otimes \mathbf{I}_n$ . The properties of the Kronecker product (fact (14)) ensures us that  $\forall \mathbf{M}, \mathbf{N}, \tilde{\mathbf{M}}\tilde{\mathbf{N}} = \widetilde{\mathbf{M}\mathbf{N}}$ . We start with the expected mean :

$$\begin{aligned} \mathbf{k}_*^T \mathcal{K}^{-1} \mathbf{Y}_v &= \mathbf{H} \mathbf{Diag}(\mathbf{k}_i^T) \tilde{\mathbf{H}}^T \left[ \tilde{\mathbf{H}} \mathbf{Diag}(\mathbf{K}_i) \tilde{\mathbf{H}}^T + \tilde{\boldsymbol{\Sigma}} \right]^{-1} \mathbf{Y}_v \\ &= \mathbf{H} \mathbf{Diag}(\mathbf{k}_i^T) \tilde{\mathbf{H}}^T \left[ \tilde{\boldsymbol{\Sigma}}^{-1} - \tilde{\boldsymbol{\Sigma}}^{-1} \tilde{\mathbf{H}} \left( \mathbf{Diag}(\mathbf{K}_i^{-1}) + \tilde{\mathbf{H}}^T \tilde{\boldsymbol{\Sigma}}^{-1} \tilde{\mathbf{H}} \right)^{-1} \tilde{\mathbf{H}}^T \tilde{\boldsymbol{\Sigma}}^{-1} \right] \mathbf{Y}_v \\ &= \mathbf{H} \mathbf{Diag}(\mathbf{k}_i^T) \left[ \tilde{\mathbf{H}}^T \tilde{\boldsymbol{\Sigma}}^{-1} - \tilde{\mathbf{H}}^T \tilde{\boldsymbol{\Sigma}}^{-1} \tilde{\mathbf{H}} \left( \mathbf{Diag}(\mathbf{K}_i^{-1}) + \tilde{\boldsymbol{\Sigma}}_P^{-1} \right)^{-1} \tilde{\mathbf{H}}^T \tilde{\boldsymbol{\Sigma}}^{-1} \right] \mathbf{Y}_v \\ &= \mathbf{H} \mathbf{Diag}(\mathbf{k}_i^T) \left[ \tilde{\mathbf{I}}_q - \tilde{\boldsymbol{\Sigma}}_P^{-1} \left( \mathbf{Diag}(\mathbf{K}_i^{-1}) + \tilde{\boldsymbol{\Sigma}}_P^{-1} \right)^{-1} \right] \tilde{\mathbf{H}}^T \tilde{\boldsymbol{\Sigma}}^{-1} \mathbf{Y}_v \\ &= \mathbf{H} \mathbf{Diag}(\mathbf{k}_i^T) \left[ \tilde{\boldsymbol{\Sigma}}_P^{-1} - \tilde{\boldsymbol{\Sigma}}_P^{-1} \left[ \mathbf{Diag}(\mathbf{K}_i^{-1}) + \tilde{\boldsymbol{\Sigma}}_P^{-1} \right]^{-1} \tilde{\boldsymbol{\Sigma}}_P^{-1} \right] \tilde{\boldsymbol{\Sigma}}_P \tilde{\mathbf{H}}^T \tilde{\boldsymbol{\Sigma}}^{-1} \mathbf{Y}_v \\ &= \mathbf{H} \mathbf{Diag}(\mathbf{k}_i^T) \left[ \mathbf{Diag}(\mathbf{K}_i) + \tilde{\boldsymbol{\Sigma}}_P \right]^{-1} \tilde{\boldsymbol{\Sigma}}_P \tilde{\mathbf{H}}^T \tilde{\boldsymbol{\Sigma}}^{-1} \mathbf{vec}(\mathbf{Y}) \\ &= \mathbf{H} \mathbf{Diag}(\mathbf{k}_i^T) \left[ \mathbf{Diag}(\mathbf{K}_i) + \boldsymbol{\Sigma}_P \otimes \mathbf{I}_n \right]^{-1} \mathbf{vec}(\mathbf{Y} \boldsymbol{\Sigma}^{-1} \mathbf{H} \boldsymbol{\Sigma}_P^{-1}) \end{aligned}$$

The first equality is from the above considerations ; the second is from Woodbury's identity ; the sixth is a backward application of Woodbury's identity ; and the last is an application of fact (15).

We now turn to the expected variance, setting further notations  $\mathbb{K} = \mathbf{Diag}(\mathbf{K}_i)$  and  $\mathfrak{K} = \mathbf{Diag}(\mathbf{k}_i)$  for compacity:

$$\begin{aligned} \mathbf{k}_{**} - \mathbf{k}_*^T \mathcal{K}^{-1} \mathbf{k}_* &= \mathbf{H} \mathbf{Diag}(\mathbf{k}_{i**}) \mathbf{H}^T - \mathbf{H} \mathfrak{K}^T \tilde{\mathbf{H}}^T \left( \tilde{\mathbf{H}} \mathbb{K} \tilde{\mathbf{H}}^T + \tilde{\boldsymbol{\Sigma}} \right)^{-1} \tilde{\mathbf{H}} \mathfrak{K} \mathbf{H}^T \\ &= \mathbf{H} \left[ \mathbf{Diag}(\mathbf{k}_{i**}) - \mathfrak{K}^T \tilde{\mathbf{H}}^T \left( \tilde{\mathbf{H}} \mathbb{K} \tilde{\mathbf{H}}^T + \tilde{\boldsymbol{\Sigma}} \right)^{-1} \tilde{\mathbf{H}} \mathfrak{K} \right] \mathbf{H}^T \\ &= \mathbf{H} \left[ \mathbf{Diag}(\mathbf{k}_{i**}) - \mathfrak{K}^T \left( \mathbb{K} + \tilde{\boldsymbol{\Sigma}}_P \right)^{-1} \mathfrak{K} \right] \mathbf{H}^T \\ &= \mathbf{H} \left[ \mathbf{Diag}(k_{i**}) - \mathbf{Diag}(\mathbf{k}_{i*}^T) \left[ \mathbf{Diag}(\mathbf{K}_i) + (\mathbf{H}^T \boldsymbol{\Sigma}^{-1} \mathbf{H})^{-1} \otimes \mathbf{I}_n \right]^{-1} \mathbf{Diag}(\mathbf{k}_{i*}) \right] \mathbf{H}^T \end{aligned}$$

The first equality is from the above considerations, and the third is lemma 3.  $\square$

<sup>8</sup>This can be seen by writing explicitly the coordinates of  $\mathbf{K} = \sum_{i=1}^q \mathbf{B}_i \otimes \mathbf{K}_i$ , reminding that  $\mathbf{B}_i = \mathbf{H}_i \mathbf{H}_i^T$  (where  $\mathbf{H}_i$  is the  $i$ -th column of  $\mathbf{H}$ ).



## B.5 Proof of prop.3 to 5

Propositions 3 and 5 are proven in annexes D, E and F of Bruinsma (2020, [6]). We add a few supplementary clarifications:

- Proof of ( $\mathbf{TY}$  sufficient statistic for  $\mathbf{U}$ )  $\Rightarrow$  ( $p(\mathbf{U}|\mathbf{Y}) = p(\mathbf{U}|\mathbf{TY})$ ):

$$\begin{aligned} p(\mathbf{U}|\mathbf{Y}) &= \frac{p(\mathbf{U}, \mathbf{Y})}{p(\mathbf{Y})} = \frac{p(\mathbf{U}, \mathbf{Y}, \mathbf{TY})}{p(\mathbf{Y})} = \frac{p(\mathbf{Y}|\mathbf{TY}, \mathbf{U})p(\mathbf{TY}, \mathbf{U})}{p(\mathbf{Y})} = \frac{p(\mathbf{Y}|\mathbf{TY})p(\mathbf{TY}, \mathbf{U})}{p(\mathbf{Y})} \\ &= \frac{p(\mathbf{Y}, \mathbf{TY})p(\mathbf{TY}, \mathbf{U})}{p(\mathbf{TY})p(\mathbf{Y})} = p(\mathbf{TY}|\mathbf{Y}) \frac{p(\mathbf{TY}, \mathbf{U})}{p(\mathbf{TY})} = 1 \times p(\mathbf{U}|\mathbf{TY}) \end{aligned} \quad (21)$$

where the fourth equality is precisely the definition of  $\mathbf{TY}$  being a sufficient statistic of  $\mathbf{U}$  for the data  $\mathbf{Y}$  : conditionally on  $\mathbf{TY}$ , the probability of the data doesn't depend on  $\mathbf{U}$ .

- Proof of  $\mathbf{TY}|\mathbf{U} \sim \mathcal{N}(\mathbf{U}_v, \Sigma_P \otimes \mathbf{I}_n)$  : by definition of the LMC  $\mathbf{Y}_v|\mathbf{U} \sim \mathcal{N}((\mathbf{H} \otimes \mathbf{I}_n)\mathbf{U}_v, \Sigma \otimes \mathbf{I}_n)$ , so  $p(\mathbf{TY}|\mathbf{U}) = p((\mathbf{T} \otimes \mathbf{I}_n)\mathbf{Y}_v|\mathbf{U}) = \mathcal{N}((\mathbf{T} \otimes \mathbf{I}_n)(\mathbf{H} \otimes \mathbf{I}_n)\mathbf{U}_v, \mathbf{T}\Sigma\mathbf{T}^T \otimes \mathbf{I}_n) = \mathcal{N}(\mathbf{U}_v, \Sigma_P \otimes \mathbf{I}_n)$  because  $\mathbf{TH} = \mathbf{I}_q$ .

Proof of prop.4 is essentially trivial, all involved matrices being block-diagonal if the DPN condition stands (in particular,  $\mathcal{K} = \text{Diag}(\mathbf{K}_i) + \Sigma_P \otimes \mathbf{I}_n = \text{Diag}(\mathbf{K}_i + \sigma_i^2 \mathbf{I}_n)$ ). Notice that for any block-diagonal matrix  $\tilde{\mathbf{D}} = \text{Diag}(\mathbf{D}_i)$  and any matrix  $\mathbf{M}$  such that the blocksize of  $\tilde{\mathbf{D}}$  matches the column size of  $\mathbf{M}$ , we have  $\tilde{\mathbf{D}} \text{vec}(\mathbf{M}) = \text{Diag}(\mathbf{D}_i \mathbf{M}_i)$ , where  $\mathbf{M}_i$  is the  $i$ -th column of  $\mathbf{M}$ ; this explains the  $\mathbf{T}_i$ 's present in the final expression.

## B.6 Proof of prop.6 to 8

**Lemma 1.** Any symmetric matrix  $\mathcal{S}$  can be decomposed as  $\mathcal{S} = \mathbf{QAQ}^T + \mathbf{Q}_\perp \mathbf{BQ}_\perp^T + \mathbf{QCQ}_\perp^T + \mathbf{Q}_\perp \mathbf{C}^T \mathbf{Q}^T$ , with  $\mathbf{A}, \mathbf{B}$  symmetric matrices and  $\mathbf{C}$  a  $q \times (p - q)$  matrix.

*Proof.* It suffices to write that  $\mathcal{S} = (\mathbf{QQ}^T + \mathbf{Q}_\perp \mathbf{Q}_\perp^T) \mathcal{S} (\mathbf{QQ}^T + \mathbf{Q}_\perp \mathbf{Q}_\perp^T)$  (because  $\mathbf{QQ}^T$  and  $\mathbf{Q}_\perp \mathbf{Q}_\perp^T$  are supplementary orthogonal projectors), and then set  $\mathbf{A} = \mathbf{Q}^T \mathcal{S} \mathbf{Q}$ ,  $\mathbf{B} = \mathbf{Q}_\perp^T \mathcal{S} \mathbf{Q}_\perp$ ,  $\mathbf{C} = \mathbf{Q}^T \mathcal{S} \mathbf{Q}_\perp$ . Another way of seeing this is by noticing that  $\mathbf{A}$ ,  $\mathbf{B}$ ,  $\mathbf{C}$  and  $\mathbf{C}^T$  are the blocks of the representation of  $\mathcal{S}$  in the basis spanned by  $\mathbf{Q}$  and  $\mathbf{Q}_\perp$ .  $\square$

**Proposition 6.** Let  $\Sigma^{-1} = \mathbf{QAQ}^T + \mathbf{Q}_\perp \mathbf{BQ}_\perp^T + \mathbf{QCQ}_\perp^T + \mathbf{Q}_\perp \mathbf{C}^T \mathbf{Q}^T$  be a decomposition of  $\Sigma^{-1}$  as in lemma 1. Then  $\Sigma_P = \mathbf{R}^{-1} \mathbf{A}^{-1} \mathbf{R}^{-T}$ , (where  $\mathbf{R}^{-T}$  denotes the inverse transpose of  $\mathbf{R}$ ) and the DPN condition is equivalent to  $(\mathbf{A} = \mathbf{R}^{-T} \mathbf{D} \mathbf{R}^{-1})$  for some diagonal matrix  $\mathbf{D}$  of size  $q$ .

*Proof.* We have  $\mathbf{H}^T \Sigma^{-1} \mathbf{H} = \mathbf{R}^T \mathbf{Q}^T \Sigma^{-1} \mathbf{Q} \mathbf{R}$ ; moreover,  $\mathbf{Q}^T \mathbf{Q}_\perp = \mathbf{0}$ ,  $\mathbf{Q}_\perp^T \mathbf{Q} = \mathbf{0}$  and  $\mathbf{Q}^T \mathbf{Q} = \mathbf{I}_q$  because the columns of  $\mathbf{Q}$  and  $\mathbf{Q}_\perp$  are mutually orthonormal. Thus we see that the only term from the decomposition of  $\Sigma^{-1}$  that is preserved by left- and right-multiplication by  $\mathbf{Q}$  and  $\mathbf{Q}^T$  is  $\mathbf{A}$  :  $\mathbf{H}^T \Sigma^{-1} \mathbf{H} = \mathbf{R}^T \mathbf{A} \mathbf{R} \Leftrightarrow \Sigma_P = \mathbf{R}^{-1} \mathbf{A}^{-1} \mathbf{R}^{-T}$ . Moreover,  $(\mathbf{H}^T \Sigma^{-1} \mathbf{H} \text{ is diagonal}) \Leftrightarrow (\mathbf{R}^T \mathbf{A} \mathbf{R} = \mathbf{D} \text{ for some diagonal matrix } \mathbf{D}) \Leftrightarrow (\mathbf{A} = \mathbf{R}^{-T} \mathbf{D} \mathbf{R}^{-1} \text{ for some diagonal matrix } \mathbf{D})$ .  $\square$

**Proposition 7.** Given its above decomposition, the following factorized decomposition stands for any symmetric matrix  $\Sigma^{-1}$  :

$$\Sigma^{-1} = \mathbf{Q}_+ \mathbf{R}_+^{-T} \mathbf{D}_+^{-1} \mathbf{R}_+^{-1} \mathbf{Q}_+^T, \quad (22)$$

where :  $\mathbf{Q}_+ = \left( \begin{array}{c|c} \mathbf{Q} & \mathbf{Q}_\perp \end{array} \right)$ ,  $\mathbf{R}_+ = \left( \begin{array}{c|c} \mathbf{R} & \mathbf{0} \\ \hline \mathbf{0} & \mathbf{I}_{p-q} \end{array} \right)$ ,  $\mathbf{D}_+^{-1} = \left( \begin{array}{c|c} \mathbf{D} & \mathbf{M} \\ \hline \mathbf{M}^T & \mathbf{B} \end{array} \right)$ ,  $\mathbf{D} = \mathbf{R}^T \mathbf{A} \mathbf{R}$  and  $\mathbf{M} = \mathbf{R}^T \mathbf{C}$ . Note that by construction  $\mathbf{Q}_+$  is a  $p \times p$  orthonormal matrix and  $\mathbf{R}_+$  is a  $p \times p$  upper triangular matrix. By prop.6,  $\mathbf{D} = \Sigma_P^{-1}$ , so it is diagonal if and only if the DPN condition stands.

*Proof.* The proof is by direct calculation. Starting from the suggested factorized form, one easily arrives at :  $\mathbf{Q}_+ \mathbf{R}_+^{-T} \mathbf{D}_+^{-1} \mathbf{R}_+^{-1} \mathbf{Q}_+^T = \mathbf{Q} \mathbf{R}^{-T} \mathbf{D} \mathbf{R}^{-1} \mathbf{Q}^T + \mathbf{Q}_\perp \mathbf{B} \mathbf{Q}_\perp^T + 2 \text{Sym}(\mathbf{Q} \mathbf{R}^{-T} \mathbf{M} \mathbf{Q}_\perp^T)$ . From this, we can identify terms with the above additive decomposition (where every identification is valid), which yields the announced formulas for  $\mathbf{D}$  and  $\mathbf{M}$ .  $\square$

**Lemma 4.** The blockwise inversion matrix formulas yield the following relations between our "regular" variables and their tilded counterparts :

$$\tilde{\mathbf{D}} = (\mathbf{D} - \mathbf{M} \mathbf{B}^{-1} \mathbf{M}^T)^{-1} ; \tilde{\mathbf{B}} = (\mathbf{B} - \mathbf{M}^T \mathbf{D}^{-1} \mathbf{M})^{-1} ; \mathbf{M} = -\mathbf{D} \tilde{\mathbf{M}} \tilde{\mathbf{B}}^{-1} ; \tilde{\mathbf{M}} = -\tilde{\mathbf{D}} \mathbf{M} \mathbf{B}. \quad (23)$$



All this parametrization also yields valuable insight about the model. For instance, we have the following expressions for  $\mathbf{T}$  :

**Proposition 8.**

$$\mathbf{T} = \mathbf{H}^+ + \Sigma_{\mathbf{P}} \mathbf{H}^T \mathbf{Q} \mathbf{C} \mathbf{Q}_{\perp}^T = \mathbf{H}^+ + \Sigma_{\mathbf{P}} \mathbf{H}^T \mathbf{P} \Sigma^{-1} \mathbf{P}_{\perp}^T \quad (24)$$

$$\mathbf{T} = \mathbf{H}^+ (\mathbf{I}_{\mathbf{P}} - \Sigma \mathbf{Q}_{\perp} \tilde{\mathbf{B}}^{-1} \mathbf{Q}_{\perp}^T) = \mathbf{H}^+ (\mathbf{I}_{\mathbf{P}} - \Sigma \mathbf{Q}_{\perp} (\mathbf{Q}_{\perp}^T \Sigma \mathbf{Q}_{\perp})^{-1} \mathbf{Q}_{\perp}^T) \quad (25)$$

where  $\mathbf{H}^+$  is the Moore-Penrose pseudoinverse of  $\mathbf{H}$ , and  $\mathbf{P} = \mathbf{Q} \mathbf{Q}^T$  and  $\mathbf{P}_{\perp} = \mathbf{Q}_{\perp} \mathbf{Q}_{\perp}^T$  are the orthogonal projectors on respectively  $\text{Span}(\mathbf{Q})$  and  $\text{Span}(\mathbf{Q}_{\perp}) = \text{Span}(\mathbf{Q})^{\perp}$ . The second equality of each line aim at showing that these expressions don't depend on a particular choice of the orthogonal complement  $\mathbf{Q}_{\perp}$ .

*Proof.* We recall from prop.6 that  $\Sigma_{\mathbf{P}} = \mathbf{D}^{-1}$ . Applying  $\mathbf{H}^T$  to the additive decomposition of  $\Sigma^{-1}$  strikes out the terms beginning with  $\mathbf{Q}_{\perp}$ , so :

$$\mathbf{T} = \Sigma_{\mathbf{P}} \mathbf{H}^T \Sigma^{-1} = \Sigma_{\mathbf{P}} \mathbf{R}^T \mathbf{Q}^T (\mathbf{Q} \mathbf{A} \mathbf{Q}^T + \mathbf{Q}_{\perp} \mathbf{B} \mathbf{Q}_{\perp}^T + \mathbf{Q} \mathbf{C} \mathbf{Q}_{\perp}^T + \mathbf{Q}_{\perp} \mathbf{C}^T \mathbf{Q}^T) = \Sigma_{\mathbf{P}} \mathbf{R}^T \mathbf{A} \mathbf{Q}^T + \Sigma_{\mathbf{P}} \mathbf{R}^T \mathbf{C} \mathbf{Q}_{\perp}^T.$$

The first term is equal to  $\Sigma_{\mathbf{P}} \mathbf{R}^T (\mathbf{R}^{-T} \mathbf{D} \mathbf{R}^{-1}) \mathbf{Q}^T = \mathbf{D}^{-1} \mathbf{D} \mathbf{R}^{-1} \mathbf{Q}^T = \mathbf{H}^+$  (the latter equality being a standard result about the Moore-Penrose pseudoinverse). We can bring the second term in two directions, that yield each line on the results. In the first one,  $\Sigma_{\mathbf{P}} \mathbf{R}^T \mathbf{C} \mathbf{Q}_{\perp}^T = \Sigma_{\mathbf{P}} \mathbf{R}^T \mathbf{Q}^T \mathbf{Q} \mathbf{C} \mathbf{Q}_{\perp}^T = \Sigma_{\mathbf{P}} \mathbf{H}^T \mathbf{Q} (\mathbf{Q}^T \Sigma^{-1} \mathbf{Q}_{\perp}) \mathbf{Q}_{\perp}^T = \Sigma_{\mathbf{P}} \mathbf{H}^T \mathbf{P} \Sigma^{-1} \mathbf{P}_{\perp}^T$ . In the second one,

$$\begin{aligned} \Sigma_{\mathbf{P}} \mathbf{R}^T \mathbf{C} \mathbf{Q}_{\perp}^T &= \Sigma_{\mathbf{P}} \mathbf{R}^T (\mathbf{R}^{-T} \mathbf{M}) \mathbf{Q}_{\perp}^T = \mathbf{D}^{-1} \mathbf{M} \mathbf{Q}_{\perp}^T = \mathbf{D}^{-1} (-\tilde{\mathbf{D}} \tilde{\mathbf{M}} \tilde{\mathbf{B}}^{-1}) \mathbf{Q}_{\perp}^T \\ &= -(\mathbf{R}^{-1} \tilde{\mathbf{C}}) \tilde{\mathbf{B}}^{-1} \mathbf{Q}_{\perp}^T = -\mathbf{R}^{-1} (\mathbf{Q}^T \Sigma \mathbf{Q}_{\perp}) \tilde{\mathbf{B}}^{-1} \mathbf{Q}_{\perp}^T \\ &= -\mathbf{H}^+ \Sigma \mathbf{Q}_{\perp} \tilde{\mathbf{B}}^{-1} \mathbf{Q}_{\perp}^T = -\mathbf{H}^+ \Sigma \mathbf{Q}_{\perp} (\mathbf{Q}_{\perp}^T \Sigma \mathbf{Q}_{\perp})^{-1} \mathbf{Q}_{\perp}^T \end{aligned}$$

where the equality  $\mathbf{M} = -\tilde{\mathbf{D}} \tilde{\mathbf{M}} \tilde{\mathbf{B}}^{-1}$  is from lemma 4 and the other are from the definitions of the variables.

Seing that these expressions are invariant to the choice of  $\mathbf{Q}_{\perp}$  is obvious for the first line :  $\mathbf{P}_{\perp} = \mathbf{Q}_{\perp} \mathbf{Q}_{\perp}^T$  is only one possible expression of the orthogonal projector on  $\text{Span}(\mathbf{Q})^{\perp}$ , the orthogonal supplementary of  $\text{Span}(\mathbf{Q})$ . It's slightly less obvious for the second line : to see it, recall that any orthonormal complement of  $\mathbf{Q}$  denoted as  $\mathbf{Q}'$  can be written  $\mathbf{Q}' = \mathbf{Q}_{\perp} \mathbf{W}$  for some square orthonormal matrix  $\mathbf{W}$ . Then :  $\mathbf{Q}' (\mathbf{Q}'^T \Sigma \mathbf{Q}')^{-1} \mathbf{Q}'^T = \mathbf{Q}_{\perp} \mathbf{W} (\mathbf{W}^T \mathbf{Q}_{\perp}^T \Sigma \mathbf{Q}_{\perp} \mathbf{W})^{-1} \mathbf{W}^T \mathbf{Q}_{\perp}^T = \mathbf{Q}_{\perp} \mathbf{W} \mathbf{W}^T (\mathbf{Q}_{\perp}^T \Sigma \mathbf{Q}_{\perp})^{-1} \mathbf{W} \mathbf{W}^T \mathbf{Q}_{\perp}^T = \mathbf{Q}_{\perp} (\mathbf{Q}_{\perp}^T \Sigma \mathbf{Q}_{\perp})^{-1} \mathbf{Q}_{\perp}^T$ .  $\square$

## B.7 Proof of prop.9 and 10

**Proposition 9.**

$$-2 \log p(\mathbf{Y}) = (p-q)n \log 2\pi + 2n \log |\mathbf{R}| + n \log |\tilde{\mathbf{B}}| + \text{Tr}(\mathbf{Y} \mathbf{Q}_{\perp} \tilde{\mathbf{B}}^{-1} \mathbf{Q}_{\perp}^T \mathbf{Y}^T) + \sum_{i=1}^q \log \mathcal{N}(\mathbf{Y} \mathbf{T}_i | \mathbf{0}, \mathbf{K}_i + \sigma_i \mathbf{I}_n) \quad (26)$$

$\tilde{\mathbf{B}}^{-1}$ ,  $\Sigma_{\mathbf{P}}$  and  $\mathbf{M}$  (present in this expression through  $\mathbf{T}$ ) form a full parametrization of the transformed noise matrix  $\mathbf{D}_+$  and can be optimized independently.

*Proof.* We start from an intermediary expression taken from the appendix G of Bruinsma (2020, [6]) under the DPN hypothesis :

$$-2 \log p(\mathbf{Y}) = (p-q)n \log 2\pi + n \log \frac{|\Sigma|}{|\Sigma_{\mathbf{P}}|} + \sum_{j=1}^n \mathbf{Y}_j (\Sigma^{-1} - \mathbf{T}^T \Sigma_{\mathbf{P}}^{-1} \mathbf{T}) \mathbf{Y}_j^T + \sum_{i=1}^q \log \mathcal{N}(\mathbf{Y} \mathbf{T}_i | \mathbf{0}, \mathbf{K}_i + \sigma_i \mathbf{I}_n) \quad (27)$$

where the second term represents the noise lost by projection, the third is the data lost by projection and the last is the standard GP MLL of the independent latent processes. Plugging in the factorization of prop.7, we just reformulate the second and third terms on the right-hand size. Let's start with the second, corresponding to the discarded noise : using the quantities from the previous section, it suffices to note that with the suggested factorization  $|\Sigma| = |\mathbf{R}|^2 |\mathbf{D}_+|$ . Then, by Schur's determinant formula (determinant of a four-blocks matrix),  $|\mathbf{D}_+| = |\tilde{\mathbf{B}}| |\tilde{\mathbf{D}} - \tilde{\mathbf{M}} \tilde{\mathbf{B}}^{-1} \mathbf{M}^T| = |\tilde{\mathbf{B}}| |\Sigma_{\mathbf{P}}|$ . We now address the third term. The proof of (8) shows that



$\mathbf{H}^T \Sigma^{-1} = \Sigma_{\mathbf{P}}^{-1} \mathbf{T} = \Sigma_{\mathbf{P}}^{-1} \mathbf{R}^{-1} \mathbf{Q}^T + \mathbf{M} \mathbf{Q}_{\perp}^T$ , so :

$$\begin{aligned}
\Sigma^{-1} - \mathbf{T}^T \Sigma_{\mathbf{P}}^{-1} \mathbf{T} &= \Sigma^{-1} - \Sigma^{-1} \mathbf{H} \Sigma_{\mathbf{P}} \mathbf{H}^T \Sigma^{-1} \\
&= \Sigma^{-1} - (\mathbf{Q} \mathbf{R}^{-T} \Sigma_{\mathbf{P}}^{-1} + \mathbf{Q}_{\perp} \mathbf{M}^T) \Sigma_{\mathbf{P}} (\Sigma_{\mathbf{P}}^{-1} \mathbf{R}^{-1} \mathbf{Q}^T + \mathbf{M} \mathbf{Q}_{\perp}^T) \\
&= \Sigma^{-1} - \mathbf{Q}_{+} \left( \frac{\mathbf{R}^{-T} \Sigma_{\mathbf{P}}^{-1} \Sigma_{\mathbf{P}} \Sigma_{\mathbf{P}}^{-1} \mathbf{R}^{-1}}{\mathbf{M}^T \Sigma_{\mathbf{P}} \Sigma_{\mathbf{P}}^{-1} \mathbf{R}^{-1}} \middle| \frac{\mathbf{R}^{-T} \Sigma_{\mathbf{P}}^{-1} \Sigma_{\mathbf{P}} \mathbf{M}}{\mathbf{M}^T \Sigma_{\mathbf{P}} \mathbf{M}} \right) \mathbf{Q}_{+}^T \\
&= \mathbf{Q}_{+} \mathbf{R}_{+}^{-T} \left( \frac{\Sigma_{\mathbf{P}}^{-1}}{\mathbf{M}^T} \middle| \frac{\mathbf{M}}{\mathbf{B}} \right) \mathbf{R}_{+}^{-1} \mathbf{Q}_{+}^T - \mathbf{Q}_{+} \mathbf{R}_{+}^{-T} \left( \frac{\Sigma_{\mathbf{P}}^{-1}}{\mathbf{M}^T} \middle| \frac{\mathbf{M}}{\mathbf{M}^T \Sigma_{\mathbf{P}} \mathbf{M}} \right) \mathbf{R}_{+}^{-1} \mathbf{Q}_{+}^T \\
&= \mathbf{Q}_{\perp} (\mathbf{B} - \mathbf{M}^T \Sigma_{\mathbf{P}} \mathbf{M}) \mathbf{Q}_{\perp}^T \\
&= \mathbf{Q}_{\perp} \tilde{\mathbf{B}}^{-1} \mathbf{Q}_{\perp}^T \quad \text{by blockwise inversion formula.}
\end{aligned}$$

It remains to prove that  $\tilde{\mathbf{B}}$ ,  $\Sigma_{\mathbf{P}}$  and  $\mathbf{M}$  form a proper parametrization of  $\Sigma$ . First notice that  $\tilde{\mathbf{B}}$  is the Schur complement of  $\Sigma_{\mathbf{P}}$  inside  $\mathbf{D}_{+}$ . It happens that providing a pair of Schur complements of a symmetric matrix and any diagonal block of itself or its inverse fully specifies this matrix. Indeed, using the previous tilded notations for the blocks of  $\Sigma$ , blockwise matrix inversion formulas show that  $\tilde{\mathbf{D}} = \Sigma_{\mathbf{P}} + \Sigma_{\mathbf{P}} \mathbf{M} \tilde{\mathbf{B}} \mathbf{M}^T \Sigma_{\mathbf{P}}$ ,  $\tilde{\mathbf{M}} = -\Sigma_{\mathbf{P}} \mathbf{M} \tilde{\mathbf{B}}$ , and finally  $\mathbf{B} = \tilde{\mathbf{B}}^{-1} + \tilde{\mathbf{B}}^{-1} \tilde{\mathbf{M}}^T \Sigma_{\mathbf{P}}^{-1} \tilde{\mathbf{M}} \tilde{\mathbf{B}}^{-1}$ , so that by the last equality  $\mathbf{B} = \tilde{\mathbf{B}}^{-1} + \mathbf{M}^T \Sigma_{\mathbf{P}} \mathbf{M}$ . Thus we see that all blocks of  $\Sigma^{-1}$  and  $\Sigma$  are expressed from  $\tilde{\mathbf{B}}$ ,  $\Sigma_{\mathbf{P}}$  and  $\mathbf{M}$  without any circular definitions.  $\square$

**Proposition 10.** *The projection matrix  $\mathbf{T}$  and posteriors of the model don't depend on  $\tilde{\mathbf{B}}$  ; moreover,  $\tilde{\mathbf{B}}$  can be restricted to be diagonal without incidence on the likelihood.*

*Proof.* Prop.2 shows that the estimated mean and variance depend on  $\Sigma$  through  $\mathbf{T}$  and  $\Sigma_{\mathbf{P}}$  only. Prop.9 states that  $(\tilde{\mathbf{B}}, \Sigma_{\mathbf{P}}, \mathbf{M})$  is a complete and independent parametrization of  $\Sigma$ , so  $\mathbf{T} = \mathbf{R}^{-1} \mathbf{Q}^T + \Sigma_{\mathbf{P}} \mathbf{M} \mathbf{Q}_{\perp}^T$  (see prop.8) doesn't depend on  $\tilde{\mathbf{B}}$  and neither do the posteriors.

For the second affirmation, notice that the likelihood is invariant under the transformation  $\tilde{\mathbf{B}}^{-1} \leftarrow \mathbf{W} \tilde{\mathbf{B}}^{-1} \mathbf{W}^T$ ,  $\mathbf{Q}_{\perp} \leftarrow \mathbf{Q}_{\perp} \mathbf{W}^T$  with  $\mathbf{W}$  orthonormal, as in particular it doesn't affect  $\mathbf{T}$  (which by prop.8 only depends on  $\text{Im}(\mathbf{Q}_{\perp})$  and not a specific vector basis) ; moreover, such a transformation of  $\mathbf{Q}_{\perp}$  doesn't affect posteriors of the model either, as it only appears in  $\mathbf{T}$ . Therefore, we can always select the matrix  $\mathbf{W}$  which diagonalizes  $\tilde{\mathbf{B}}^{-1}$ , i.e we can jointly optimize  $\tilde{\mathbf{B}}$  and  $\mathbf{Q}_{\perp}$  while enforcing the diagonality of  $\tilde{\mathbf{B}}$ .  $\square$

## B.8 Alternate expression of the likelihood

We here propose an expression for the marginal log-likelihood inspired by [9]. It's less convenient than this of prop.9 as it doesn't boil down to MLLs of single-output GPs, but it shows that a latent-revealing expression which decouples under the DPN hypothesis can be obtained from elementary manipulations.

**Proposition 11.**

$$\begin{aligned}
-2 \log p(\mathbf{Y}) &= \sum_{j=1}^n \mathbf{Y}_j \Sigma^{-1} \mathbf{Y}_j^T - \text{vec}(\mathbf{Y}^T \Sigma^{-1} \mathbf{H})^T (\text{Diag}(\mathbf{K}_i^{-1}) + \Sigma_{\mathbf{P}}^{-1} \otimes \mathbf{I}_n)^{-1} \text{vec}(\mathbf{Y}^T \Sigma^{-1} \mathbf{H}) \\
&\quad + \log |\text{Diag}(\mathbf{K}_i) + \Sigma_{\mathbf{P}} \otimes \mathbf{I}_n| + 2n \log |\mathbf{R}| + n \log |\tilde{\mathbf{B}}| + np \log 2\pi
\end{aligned}$$

where  $\mathbf{Y}_j$  is the  $j$ -th column of  $\mathbf{Y}$ . The DPN condition is necessary and sufficient for this expression to decouple between latent processes: it then holds  $|\text{Diag}(\mathbf{K}_i) + \Sigma_{\mathbf{P}} \otimes \mathbf{I}_n| = \prod_{i=1}^q |\mathbf{K}_i + \sigma_i \mathbf{I}_n|$ , and

$$\text{vec}(\mathbf{Y}^T \Sigma^{-1} \mathbf{H})^T (\text{Diag}(\mathbf{K}_i^{-1}) + \Sigma_{\mathbf{P}}^{-1} \otimes \mathbf{I}_n)^{-1} \text{vec}(\mathbf{Y}^T \Sigma^{-1} \mathbf{H}) = \sum_{i=1}^q \mathbf{H}_i \Sigma^{-1} (\mathbf{K}_i^{-1} + \sigma_i^{-1} \mathbf{I}_n)^{-1} \mathbf{Y}^T \Sigma^{-1} \mathbf{H}_i^T.$$

*Proof.* We start by expressing the MLL in the most straightforward way :

$$-2 \log p(\mathbf{Y}) = \mathbf{Y}_{\mathbf{v}}^T \mathcal{K}^{-1} \mathbf{Y}_{\mathbf{v}} + \log |\mathcal{K}| + \frac{np}{2} \log \pi,$$

with  $\mathcal{K} = (\mathbf{H} \otimes \mathbf{I}_n) \text{Diag}(\mathbf{K}_i) (\mathbf{H}^T \otimes \mathbf{I}_n) + \Sigma \otimes \mathbf{I}_N$  as before. We deal with the first term by applying Wodburry's formula :



$$\begin{aligned}
\mathbf{Y}_v^T \mathcal{K}^{-1} \mathbf{Y}_v &= \mathbf{Y}_v^T (\Sigma^{-1} \otimes \mathbf{I}_n) \mathbf{Y}_v - \mathbf{Y}_v^T (\Sigma^{-1} \mathbf{H} \otimes \mathbf{I}_n) (\text{Diag}(\mathbf{K}_i^{-1}) + \Sigma_P^{-1} \otimes \mathbf{I}_n)^{-1} (\mathbf{H}^T \Sigma^{-1} \otimes \mathbf{I}_n) \mathbf{Y}_v \\
&= \sum_{j=1}^n \mathbf{Y}_j \Sigma^{-1} \mathbf{Y}_j^T - \text{vec}(\mathbf{Y}^T \Sigma^{-1} \mathbf{H})^T (\text{Diag}(\mathbf{K}_i^{-1}) + \Sigma_P^{-1} \otimes \mathbf{I}_n)^{-1} \text{vec}(\mathbf{Y}^T \Sigma^{-1} \mathbf{H})
\end{aligned}$$

For the log-determinant, we use the parametrization of section 4:

$$\begin{aligned}
|\mathcal{K}| &= |\mathbf{Q}_+ \mathbf{R}_+ \otimes \mathbf{I}_n| |\mathbf{D}_+ \otimes \mathbf{I}_n + \text{Diag}(\mathbf{K}_i)| |\mathbf{R}_+^T \mathbf{Q}_+^T \otimes \mathbf{I}_n| \\
&= |\mathbf{R}_+|^n |\mathbf{D}_+ \otimes \mathbf{I}_n + \text{Diag}(\mathbf{K}_i)| |\mathbf{R}_+|^n \quad \text{because } |\mathbf{Q}_+| = 1 \text{ and by the properties of the Kronecker product} \\
&= |\mathbf{R}|^{2n} |\tilde{\mathbf{B}} \otimes \mathbf{I}_n| \left| \left( \text{Diag}(\mathbf{K}_i) + \tilde{\mathbf{D}} \otimes \mathbf{I}_n \right) - \tilde{\mathbf{M}} \tilde{\mathbf{B}}^{-1} \tilde{\mathbf{M}}^T \otimes \mathbf{I}_n \right| \quad \text{by Schur's determinant formula} \\
&= |\mathbf{R}|^{2n} |\tilde{\mathbf{B}}|^n |\text{Diag}(\mathbf{K}_i) + (\tilde{\mathbf{D}} - \tilde{\mathbf{M}} \tilde{\mathbf{B}}^{-1} \tilde{\mathbf{M}}^T) \otimes \mathbf{I}_n| \\
&= |\mathbf{R}|^{2n} |\tilde{\mathbf{B}}|^n |\text{Diag}(\mathbf{K}_i) + \Sigma_P \otimes \mathbf{I}_n| \quad \text{by lemma 4}
\end{aligned}$$

which yields the desired result. For the second equality, note that the block decomposition of  $\mathbf{D}_+ \otimes \mathbf{I}_n + \text{Diag}(\mathbf{K}_i)$  (in blocks of size  $nq \times nq$ ,  $nq \times n(p-q)$ , etc) is  $\left( \begin{array}{c|c} \text{Diag}(\mathbf{K}_i) + \tilde{\mathbf{D}} \otimes \mathbf{I}_n & \tilde{\mathbf{M}} \otimes \mathbf{I}_n \\ \hline \tilde{\mathbf{M}}^T \otimes \mathbf{I}_n & \tilde{\mathbf{B}} \otimes \mathbf{I}_n \end{array} \right)$ .  $\square$

## Appendix C Restrictivity of the DPN hypothesis

This short paragraph aims at assessing the severity of the DPN hypothesis. It consists mainly of the following proposition :

**Proposition 12.** *Let  $\Sigma_{\text{opt}}$  the value of  $\Sigma$  which optimizes the MLL for the unconstrained LMC model. Let  $\Sigma_{\text{opt}}^{-1} = \mathbf{Q} \mathbf{A} \mathbf{Q}^T + \mathbf{Q}_\perp \mathbf{B} \mathbf{Q}_\perp^T + 2\text{Sym}(\mathbf{Q} \mathbf{C} \mathbf{Q}_\perp^T)$  be the decomposition of  $\Sigma_{\text{opt}}^{-1}$  as in prop.1. Then the minimal distance between  $\Sigma_{\text{opt}}^{-1}$  and a precision matrix compatible with the DPN hypothesis is :*

$$\min_{\Sigma_{\text{app}}} \|\Sigma_{\text{opt}}^{-1} - \Sigma_{\text{app}}^{-1}\|_F^2 = \min_{\mathbf{D}} \|\mathbf{A} - \mathbf{R}^{-T} \mathbf{D} \mathbf{R}^{-1}\|_F^2 \quad \text{subject to } \mathbf{D} \text{ positive and diagonal}, \quad (28)$$

where  $\|\cdot\|_F$  denotes the Frobenius norm. It is minimized for  $\Sigma_{\text{app}}^{-1} = \mathbf{Q} \mathbf{R}^{-T} \mathbf{D}' \mathbf{R}^{-1} \mathbf{Q}^T + \mathbf{Q}_\perp \mathbf{B} \mathbf{Q}_\perp^T + 2\text{Sym}(\mathbf{Q} \mathbf{C} \mathbf{Q}_\perp^T)$ , where  $\mathbf{D}' = \text{Diag}[(\mathbf{R}^{-1} \mathbf{R}^{-T} \odot \mathbf{R}^{-1} \mathbf{R}^{-T})^{-1} \text{diag}(\mathbf{R}^{-1} \mathbf{A} \mathbf{R}^{-T})]$  is the optimal  $\mathbf{D}$  in the above expression,  $\text{diag}$  is the operator taking the diagonal of a square matrix (into vector form) and  $\odot$  denotes the Hadamard product (elementwise matrix product).

*Proof.* Let's write  $\Sigma_{\text{app}}^{-1} = \mathbf{Q} \mathbf{A}' \mathbf{Q}^T + \mathbf{Q}_\perp \mathbf{B}' \mathbf{Q}_\perp^T + 2\text{Sym}(\mathbf{Q} \mathbf{C}' \mathbf{Q}_\perp^T)$  the decomposition of  $\Sigma_{\text{app}}^{-1}$ . It is a general property that the Frobenius norm of a symmetric matrix can be computed blockwise, that is :

$$\min_{\Sigma_{\text{app}}} \|\Sigma_{\text{opt}}^{-1} - \Sigma_{\text{app}}^{-1}\|_F^2 = \text{Tr}((\Sigma_{\text{opt}}^{-1} - \Sigma_{\text{app}}^{-1})^2) = \text{Tr}((\mathbf{A} - \mathbf{A}')^2) + \text{Tr}((\mathbf{B} - \mathbf{B}')^2) + 2 \text{Tr}((\mathbf{C} - \mathbf{C}')(\mathbf{C} - \mathbf{C}')^T)$$

This can be shown either by writing the norm as a sum of squared coefficients and splitting the sum at the right indices, or by replacing  $\Sigma_{\text{opt}}^{-1}$  and  $\Sigma_{\text{app}}^{-1}$  by their decompositions, expanding the trace of their squared difference and eliminating all cross-coefficients because of the circularity of the trace (i.e :  $\text{Tr}(\mathbf{Q} \mathbf{X} \mathbf{Q}_\perp^T) = \text{Tr}(\mathbf{X} \mathbf{Q}_\perp^T \mathbf{Q}) = 0$ ).

Also recall that the trace is conjugation-invariant :  $\text{Tr}(\mathbf{Q}(\mathbf{A} - \mathbf{A}')^2 \mathbf{Q}^T) = \text{Tr}((\mathbf{A} - \mathbf{A}')^2)$ , etc.

Prop. 6 showed that the DPN hypothesis doesn't put any constraints on  $\mathbf{B}$  and  $\mathbf{C}$ . Therefore, one can simply set  $\mathbf{B}' = \mathbf{B}$  and  $\mathbf{C}' = \mathbf{C}$  to zero their contribution to the discrepancy. Proposition 6 also shows that the DPN hypothesis is equivalent to  $(\mathbf{A}' = \mathbf{R}^{-T} \mathbf{D} \mathbf{R}^{-1} \text{ for some diagonal matrix } \mathbf{D})$ , hence equation (28).

In order to find the optimal  $\mathbf{D}$ , we set additional notations :  $\mathbf{D} = \text{Diag}(\mathbf{v})$  ;  $\|\mathbf{A} - \mathbf{R}^{-T} \mathbf{D} \mathbf{R}^{-1}\|_F^2 = \|\Delta\|_F^2 = \Phi(\Delta)$ ;  $\mathbf{M} : \mathbf{N} = \text{Tr}(\mathbf{M}^T \mathbf{N})$  denotes the Frobenius scalar product. We then compute the differential, considering  $\mathbf{v}$  as the only variable:

$$\begin{aligned}
d\Phi &= 2 \Delta : d\Delta = 2 \Delta : d(\mathbf{R}^{-T} \text{Diag}(\mathbf{v}) \mathbf{R}^{-1}) = 2 \Delta : \mathbf{R}^{-T} d(\text{Diag}(\mathbf{v})) \mathbf{R}^{-1} \\
&= 2 \mathbf{R}^{-1} \Delta \mathbf{R}^{-T} : d(\text{Diag}(\mathbf{v})) = 2 \mathbf{R}^{-1} \Delta \mathbf{R}^{-T} : \text{Diag}(d\mathbf{v}) = 2 \text{diag}(\mathbf{R}^{-1} \Delta \mathbf{R}^{-T}) : d\mathbf{v}
\end{aligned}$$

All of these expressions are standard manipulations involving differentials and scalar products; see for instance Petersen (2012, [20]). The last one,  $\mathbf{X} : \text{Diag}(\mathbf{y}) = \text{diag}(\mathbf{X}) : \mathbf{y}$  - where we recall that  $\text{diag}(\mathbf{X})$  denotes the



diagonal of matrix  $\mathbf{X}$  while  $\mathbf{Diag}(\mathbf{y})$  is the diagonal square matrix made from the vector  $\mathbf{y}$ , is less standard : it can be proved by direct expansion in matrix coefficients.

The last expression defines the gradient of  $\Phi$  with respect to the vector  $\mathbf{v}$  :  $\mathbf{d}\Phi = \mathbf{2} \mathbf{diag}(\mathbf{R}^{-1}\Delta\mathbf{R}^{-\mathbf{T}}) : \mathbf{d}\mathbf{v} \Leftrightarrow \nabla_{\mathbf{v}}\Phi = \mathbf{diag}(\mathbf{R}^{-1}\Delta\mathbf{R}^{-\mathbf{T}})$ . We can then set this gradient to zero to find the global minimum :

$$\begin{aligned} \nabla_{\mathbf{v}}\Phi = \mathbf{0} &\Leftrightarrow \mathbf{diag}(\mathbf{R}^{-1}\Delta\mathbf{R}^{-\mathbf{T}}) = \mathbf{0} \Leftrightarrow \mathbf{diag}(\mathbf{R}^{-1}\mathbf{A}\mathbf{R}^{-\mathbf{T}}) = \mathbf{diag}(\mathbf{R}^{-1}\mathbf{R}^{-\mathbf{T}}\mathbf{Diag}(\mathbf{v})\mathbf{R}^{-1}\mathbf{R}^{-\mathbf{T}}) \\ &\Leftrightarrow \mathbf{diag}(\mathbf{R}^{-1}\mathbf{A}\mathbf{R}^{-\mathbf{T}}) = ((\mathbf{R}^{-1}\mathbf{R}^{-\mathbf{T}}) \odot (\mathbf{R}^{-1}\mathbf{R}^{-\mathbf{T}})) \mathbf{v} \\ &\Leftrightarrow \mathbf{v} = (\mathbf{R}^{-1}\mathbf{R}^{-\mathbf{T}} \odot \mathbf{R}^{-1}\mathbf{R}^{-\mathbf{T}})^{-1} \mathbf{diag}(\mathbf{R}^{-1}\mathbf{A}\mathbf{R}^{-\mathbf{T}}) \end{aligned}$$

The second-to-last equivalence is from another unusual matrix identity :  $\mathbf{diag}(\mathbf{X}\mathbf{Diag}(\mathbf{v})\mathbf{Y}) = (\mathbf{Y}^{\mathbf{T}} \odot \mathbf{X})\mathbf{v}$ . Here again, the proof is by direct expansion of the matrix coefficients. □

Proposition 12 proves what was previously stated in a more informal way : the discrepancy between the DPN-restricted model and the unrestricted one lies only in an approximation of the "true" matrix  $\mathbf{A}$ . The fact that the minimizer of this discrepancy has a simple form paves the way for an eventual *correction procedure* for the noise : if the data is assumed to exhibit a specific noise structure which is not diagonally projectable, one could parametrize such an optimal noise  $\Sigma_{\text{opt}}$  in addition to the noise parameters  $\tilde{\mathbf{B}}$ ,  $\mathbf{M}$  and  $\Sigma_{\mathbf{P}}$  of the previous section. One would then add to the likelihood a term proportional to  $n \times \mathbf{diag}(\mathbf{R}^{-1}(\mathbf{Q}^{\mathbf{T}}\Sigma_{\text{opt}}^{-1}\mathbf{Q} - \mathbf{R}^{-\mathbf{T}}\Sigma_{\mathbf{P}}^{-1}\mathbf{R}^{-1})\mathbf{R}^{-\mathbf{T}})$  (reminding that  $\mathbf{D} = \Sigma_{\mathbf{P}}^{-1}$  and  $\mathbf{A} = \mathbf{Q}^{\mathbf{T}}\Sigma^{-1}\mathbf{Q}$ ), which would warp the model towards a more realistic noise.

Alternately, an interleaved optimization scheme could be developed, in the spirit of a projected gradient descent: at each iteration, one would estimate a DPN-compatible noise  $\Sigma_{\text{app}}$  by optimizing the MLL of prop.9, find the nearest noise  $\Sigma_{\text{opt}}$  (or at least a near one) enforcing the desired noise structure, compute its decomposition in terms of  $\mathbf{A}$ ,  $\mathbf{B}$  and  $\mathbf{C}$ , and then come back to the initial variables by setting  $\mathbf{B} \leftarrow \mathbf{B}$ ,  $\mathbf{C} \leftarrow \mathbf{C}$  and  $\Sigma_{\mathbf{P}}^{-1} = \mathbf{Diag}(\mathbf{v}) \leftarrow \mathbf{Diag}[(\mathbf{R}^{-1}\mathbf{R}^{-\mathbf{T}} \odot \mathbf{R}^{-1}\mathbf{R}^{-\mathbf{T}})^{-1} \mathbf{diag}(\mathbf{R}^{-1}\mathbf{A}\mathbf{R}^{-\mathbf{T}})]$ . This is beyond the scope of this article and has not been experimented on yet, by lack of a relevant study case.

## Appendix D Experimental specifications

### D.1 Training protocol

For each model described in the main body of the article, the training dynamics were investigated individually in order to verify that performance discrepancies weren't due to improper convergence. Modifications were tried out on the following items:

- The optimizer, between algorithms Adam, RAdam, NAdam, AdamW, SGD and LBFGS of the `torch.optim` package (Paszke, 2019, [19]);
- The learning rate scheduler, between none, exponential decay, cosine annealing, and reduction upon arrival at a plateau (all implementations also taken from `torch.optim`);
- The maximal learning rate, over the range  $[10^{-3}; 10^{-1}]$ ;
- The maximal-to-minimal learning rate ratio, over a range of 1 to 100;
- The presence or absence of a stopping criterion, defined as an early stop when differences between consecutive values of the loss remain smaller (in absolute value) to a given threshold  $\delta\mathcal{L}$  during a given number of iterations  $N_{\text{patience}}$ ;
- The values of  $\delta\mathcal{L}$  and  $N_{\text{patience}}$  if applicable;
- The (maximal) number of iterations  $N_{\text{iter}}^{\text{max}}$ , over the range  $[500; 6000]$ ;
- The initialization of the LMC coefficients, between random sampling from i.i.d standard normal distributions, and setting  $\mathbf{H}_{\text{start}} = \mathbf{U}\mathbf{S}$  with  $\mathbf{Y} = \mathbf{U}\mathbf{S}\mathbf{V}^{\mathbf{T}}$  the rank- $q$  truncated SVD of the data<sup>9</sup>.

---

<sup>9</sup>Initialization of other model parameters is much less problematic: all characteristic quantities of the toy data being of unit order, setting kernel parameters to  $\sim 1$  and noise parameters to  $\sim 10^{-2}$  always yields satisfactory results.



All variations of the Adam optimizer performed about the same (for all models) and far better than the other optimizers, the best being AdamW (Loshchilov, 2019, [16]) which was thus retained. Among schedulers, only absence of scheduling<sup>10</sup> and exponential learning rate decay yielded satisfactory results, and the latter was selected for its faster convergence and slightly higher precision at the end of training; the chosen value for the decay parameter was always  $\beta = \exp(\log(lr_{max}/lr_{min})/N_{iter}^{max})$ . These methods being fixed, it appeared that for a rather large range of the remaining optimization parameters, the training loss converged monotonously for all models – with the occasional occurrence of a "jump" out of a minimal basin, quickly overcome if enough iterations remained, when the learning rate was too large or not decaying fast enough. Optimization being monotonous, the suggested stopping criterion – training termination when no progress was made for a long time – proved to be a successful strategy, giving results as good or better as fixing a large number of iterations in advance. Choosing  $lr_{max} = 10^{-2}$ ,  $lr_{min} = 10^{-3}$ ,  $\delta\mathcal{L} = 10^{-4}$  and  $N_{patience}$  then yielded near-optimal accuracy for all models and was therefore adopted for all. Lastly, even when using the stopping criterion, a realistic maximal number of iterations had to be provided in order to compute the above learning rate decay factor  $\beta$ : experimentation revealed that model performances were very insensitive to this parameter, which mostly modulated convergence speed. In the same vein, in most cases the "clever" initialization of LMC coefficients with data-derived values was unnecessary to reach the global optimum but greatly sped up convergence. We therefore chose to impose  $N_{iter}^{max} = 5000$  and SVD-based initialization for all models: the effective number of iterations provided by the stopping criterion thus became a metric to compare convergence speed between models.

## D.2 Hardware specifications

Only Table 1 in the main body of the article contains timings. The experiment behind these results was performed on a 80-CPU (2.10GHz Intel(R) Xeon(R) Gold 6230) machine, using a pure `gpytorch/pytorch/numpy` implementation.

## Appendix E Case of a "physical" mixing matrix

In this annex we describe the generation of the physically-meaningful mixing matrix mentioned in section 5.3 ("Results of the parametric study", paragraph "Advantage over OILMM"). The proposed mechanism is as follows: each latent process represents a wave signal emitted from a point source. Each task is the total signal arriving at some (punctual) sensor. Therefore, coefficient  $H_{ij}$  is the amplitude of the signal from source  $j$  arriving at sensor  $i$  :

$$H_{ij} = \frac{A_j}{d_{ij}^2}, \quad (29)$$

where  $d_{ij}$  is the distance traveled by the wave and  $A_j$  is the signal amplitude at the location of source  $j$ . The amplitude decay in  $1/r^2$  is characteristic of light and sound waves.

The geometry of this toy model is illustrated in figure 5. The  $p$  sensors are aligned on the  $y = 0$  axis, equidistantly spaced between  $x = -1$  and  $x = 1$ . To maintain randomness, the  $q$  wave sources have random coordinates, sampled from i.i.d normal distributions with zero mean and unit variance. The last variables to specify are the  $A_j$ 's, signal amplitudes at source level: in order to make them all significant but different, we chose them to be multiples of the smallest one, i.e  $A_j = j$ .

## Appendix F Interpretation : comparison with other LMC approximations

### F.1 Relation to variational approaches

We wish to underline a link between previous results and the apparently unrelated variational methods for GPs. The latter are widespread tools to handle multitask GPs, yet the exact nature and cause of the computational gains they offer is not always clear. The focus is often on the reduction of kernel size thanks to the inducing points paradigm, and on the fact that the ELBO (approximate likelihood) factorizes over data-points. But there is another major source of gains: *variational multi-output GPs implicitly decouple latent processes*. Although a formal exposition of the variational GP framework is beyond the scope of this paper, we can show this in a few expressions using standard notations. If  $\mathbf{f}_i$  represents the values of latent process  $i$

<sup>10</sup>Other than the automatic weight decay of the Adam optimizer.



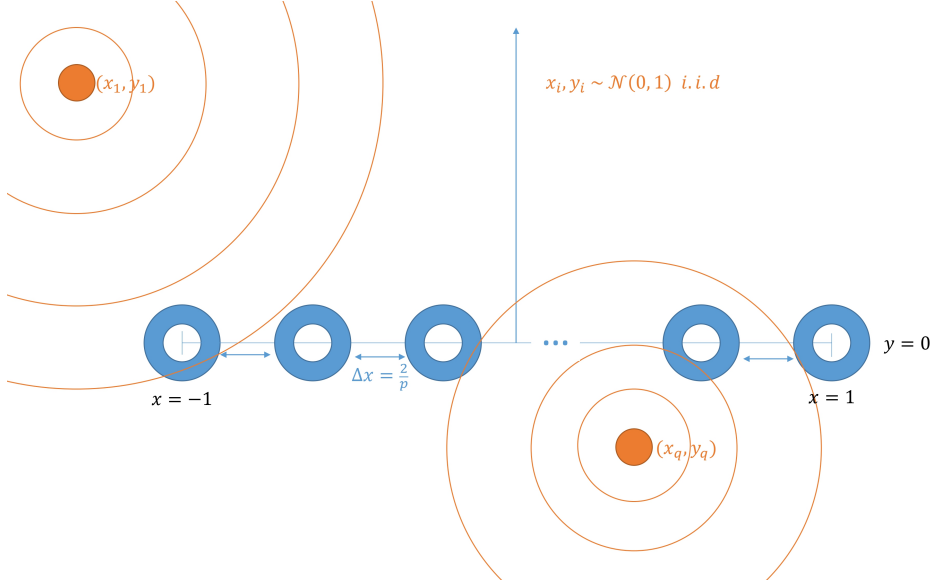


Figure 5: Geometry of the physical toy model modeled by the  $\mathbf{H}$  matrix in the last experiment of section 5.3.

at the observation points,  $\mathbf{u}_i$  its values at pseudo-input points, the approximation behind variational models is to introduce approximate posteriors  $q(\mathbf{u}_i) = \mathcal{N}(\mathbf{u}_i | \mathbf{m}_i, \mathbf{S}_i)$  ( $\mathbf{m}_i, \mathbf{S}_i$  being parameters of the model) such that  $q(\mathbf{u}_i) \simeq p(\mathbf{u}_i, \mathbf{f}_i | \mathbf{y})$ .

The key point here is that it is always assumed (but not always emphasized) that **the global approximate posterior  $q(\mathbf{u})$  factorizes over latent processes** :  $q(\mathbf{u}) = \prod_{i=1}^q q(\mathbf{u}_i)$ . This construction makes all posteriors an likelihood terms factorize too: what in the original LMC is a condition (which we have shown to be equivalent to the DPN condition) is automatically enforced in its variational counterpart.

We also wish to underline the analogy between our posterior estimators and these of the variational model, which can be found for instance in Liu (2023 [13] or 2022 [14]);  $p(\mathbf{u}_i, \mathbf{f}_i | \mathbf{y}) \simeq q(\mathbf{f}_i) = \mathcal{N}(\mu_i, \nu_i)$ , with :

$$\mu_i = \mathbf{k}_{i*}^T \mathbf{K}_i^{-1} \mathbf{m}_i \quad (30)$$

$$\nu_i = k_{i**} - \mathbf{k}_{i*}^T (\mathbf{K}_i^{-1} - \mathbf{K}_i^{-1} \mathbf{S}_i \mathbf{K}_i^{-1}) \mathbf{k}_{i*} = k_{i**} - \mathbf{k}_{i*}^T \left( \mathbf{K}_i^{-1} - \mathbf{K}_i^{-1} (\mathbf{K}_i^{-1} + (\mathbf{S}_i^{-1} - \mathbf{K}_i^{-1}))^{-1} \mathbf{K}_i^{-1} \right) \mathbf{k}_{i*} \quad (31)$$

$$= k_{i**} - \mathbf{k}_{i*}^T (\mathbf{K}_i + (\mathbf{S}_i^{-1} - \mathbf{K}_i^{-1})^{-1})^{-1} \mathbf{k}_{i*} \text{ by the previously-used Woodbury-type equality,} \quad (32)$$

where the covariance vector and matrix are here evaluated at pseudo-input points rather than observed datapoints. We notice the direct similarity with the decoupled expressions of prop.4, simply replacing  $\mathbf{Y} \mathbf{T}_i$  by  $\mathbf{m}_i$  and  $\sigma_i^2 \mathbf{I}_n$  by  $(\mathbf{S}_i^{-1} - \mathbf{K}_i^{-1})^{-1}$  (and the real observation points by their pseudo-input counterparts): **the variational model learns additional parameters** (these of the approximate posterior,  $\mathbf{m}_i$  and  $\mathbf{S}_i$ ) **which substitute themselves to the projected data and projected noise**.

## F.2 Relation to the IMC model

In this paragraph, we answer the following interrogation : are computational gains of the IMC (relative to the naive LMC implementation) due to some sort of decoupling of the latent processes ? This question seems natural, as the IMC simplifies the latent process structure compared to the LMC. However, the answer is negative : the simplification is this time of another kind.

The IMC is defined by its covariance matrix  $\mathbf{K} = \mathbf{K}_T \otimes \mathbf{K}_x$ , as opposed to this of the LMC as defined above in the matricial proof of prop.2 B.4:  $\mathbf{K} = \sum_{i=1}^q \mathbf{B}_i \otimes \mathbf{K}_i$ . This corresponds to all latent processes sharing the same kernel : if  $\mathbf{K}_i = \mathbf{K}_x \forall i$  in the latter expression, we recover the IMC by setting  $\mathbf{K}_T = \sum_{i=1}^q \mathbf{B}_i$ . As  $\mathbf{K}^{-1} = \mathbf{K}_T^{-1} \otimes \mathbf{K}_x^{-1}$  one could think that this covariance structure trivializes all computations, but this is not the case because of the noise: the noise-added covariance  $\mathcal{K} = \mathbf{K}_T \otimes \mathbf{K}_x + \mathbf{\Sigma} \otimes \mathbf{I}_n$  is still not easily invertible. Additional tricks are thus necessary to carry efficient computation ; we comment here on the approach of Rakitsch (2013, [21]), as it is exact and more efficient than the original model of Bonilla (2007, [4]) which only uses



low-rank approximations of  $\mathbf{K}_T$  and  $\mathbf{K}_x$ .

If we frame the IMC as a particular case of LMC like we did above, we get that  $\mathbf{K}_T = \mathbf{H}\mathbf{H}^T$  (because  $\mathbf{B}_i = \mathbf{H}_i\mathbf{H}_i^T$ ). We define  $\mathbf{U}_H\mathbf{S}_H^2\mathbf{U}_H^T$  as the diagonalization of  $\mathbf{K}_T$ <sup>11</sup>, and  $\mathbf{\Sigma} = \mathbf{U}_\Sigma\mathbf{S}_\Sigma\mathbf{U}_\Sigma^T$  the diagonalization of  $\mathbf{\Sigma}$ <sup>12</sup>. We can then compare our approach with this of Rakitsch (2013, [21]), which is all contained in the following decomposition (equation (7) of said paper<sup>13</sup>):

$$\mathcal{K} = \mathbf{K}_T \otimes \mathbf{K}_x + \mathbf{\Sigma} \otimes \mathbf{I}_n = \left( \mathbf{U}_\Sigma \mathbf{S}_\Sigma^{\frac{1}{2}} \otimes \mathbf{I}_n \right) \left( \mathbf{S}_\Sigma^{-\frac{1}{2}} \mathbf{U}_\Sigma^T \mathbf{K}_T \mathbf{U}_\Sigma \mathbf{S}_\Sigma^{-\frac{1}{2}} \otimes \mathbf{K}_x + \mathbf{I}_p \otimes \mathbf{I}_n \right) \left( \mathbf{S}_\Sigma^{\frac{1}{2}} \mathbf{U}_\Sigma^T \otimes \mathbf{I}_n \right) \quad (33)$$

The purpose of this factorization is to exploit the convenient properties of  $\mathbf{I}_p \otimes \mathbf{I}_n$  : indeed, for any symmetric matrices  $\mathbf{S}, \mathbf{S}'$  of eigen-decompositions  $\mathbf{U}\mathbf{D}\mathbf{U}^T$  and  $\mathbf{U}'\mathbf{D}'\mathbf{U}'^T$ , we get that the eigen-decomposition of  $(\mathbf{S} \otimes \mathbf{S}' + \mathbf{I} \otimes \mathbf{I})$  is  $(\mathbf{U} \otimes \mathbf{U}') (\mathbf{D} \otimes \mathbf{D}' + \mathbf{I} \otimes \mathbf{I}) (\mathbf{U}^T \otimes \mathbf{U}'^T)$ . The fact that the eigenvectors of the large matrix are Kronecker products authorizes easy manipulation and fast computation ; this is the approach followed by Rakitsch to perform all calculations.

On the other side, our approach relies on a different implicit factorization. For the sake of comparison, we apply it to the IMC covariance structure, which yields :

$$\mathcal{K} = \mathbf{H}\mathbf{H}^T \otimes \mathbf{K}_x + \mathbf{\Sigma} \otimes \mathbf{I}_n \simeq (\mathbf{U}_H \mathbf{S}_H \otimes \mathbf{I}_n) (\mathbf{I}_q \otimes \mathbf{K}_x + \mathbf{S}_H^{-1} \mathbf{U}_H^T \mathbf{\Sigma} \mathbf{U}_H \mathbf{S}_H^{-1} \otimes \mathbf{I}_n) (\mathbf{S}_H \mathbf{U}_H^T \otimes \mathbf{I}_n) \quad (34)$$

$$= (\mathbf{H} \otimes \mathbf{I}_n) (\mathbf{I}_q \otimes \mathbf{K}_x + \mathbf{H}^+ \mathbf{\Sigma} \mathbf{H}^{+T} \otimes \mathbf{I}_n) (\mathbf{H}^T \otimes \mathbf{I}_n), \quad (35)$$

where  $\mathbf{H}^+$  denotes the Moore-Penrose pseudoinverse of  $\mathbf{H}$ . This factorization is not rigorous as it is rank-deficient; it nonetheless appears in the matricial proof of prop.2 B.4, where is it made rigorous by two successive applications of Woodbury-like formulas involving other terms<sup>14</sup>. Besides this occurrence, factorization (35) illustrates the core of our approach : the noise-augmented covariance can be summarized by a latent block-diagonal term of size  $qn \times qn$ , left- and right-multiplied by the mixing matrix.

Comparing the above equations shows both the analogy and difference between the two approaches. Ours relies on left- and right-factorization of the the eigen-decomposition of the *task* covariance matrix; the term  $\mathbf{H}^+ \mathbf{\Sigma} \mathbf{H}^{+T}$  – in reality  $\mathbf{T} \mathbf{\Sigma} \mathbf{T}^T$  with a more rigorous derivation – has to be diagonal for the central term to be computationally efficient, hence the DPN hypothesis. On the other hand, the approach of Rakitsch factorizes the eigen-decomposition of the *noise* covariance matrix; then the central term is always easy to handle because of the  $\mathbf{I}_p \otimes \mathbf{I}_n$  term, and no additional hypothesis is necessary to attain a  $O(n^3 + p^3)$  complexity. Note however that *factorization (33) requires the GP covariance matrix to be a Kronecker product* : it is thus restricted to the IMC model.

We finally emphasize that latent processes are *not* independant conditionally on observations in the IMC: we have already shown this property to be equivalent to the DPN condition, and the present section illustrates that the DPN condition is not automatically enforced by the IMC,  $\mathbf{H}$  and  $\mathbf{\Sigma}$  still being arbitrary in this model.

<sup>11</sup>Careful inspection shows that in the IMC, if  $\mathbf{U}_H \mathbf{S}_H \mathbf{V}_H^T$  is the singular values decomposition of  $\mathbf{H}$ , it can be assumed in all generality that  $\mathbf{V}_H = \mathbf{I}_n$ , all latent processes sharing the same kernel; this is used in equation 35.

<sup>12</sup>In these definitions  $\mathbf{S}_H$  is squared for coherency with the rest of the present paper, while  $\mathbf{S}_\Sigma$  is not to keep the notations of Rakitsch [21].

<sup>13</sup>Where we have made the restriction  $\mathbf{\Omega} = \mathbf{I}_n$  for reading purposes, corresponding to homoskedastic noise.

<sup>14</sup>More exactly, in said derivation  $\mathbf{I}_q \otimes \mathbf{K}_x$  is replaced by  $\mathbf{Diag}(\mathbf{K}_i)$  (because there latent processes have different kernels), and  $\mathbf{H}^+$  is replaced by  $\mathbf{T}$ , which we recall to be another generalized inverse of  $\mathbf{H}$ .